



**UNIVERSITY
OF GÄVLE**

FACULTY OF ENGINEERING AND SUSTAINABLE DEVELOPMENT

Design of a Low-Noise Amplifier for Radar
Application in the 5 GHz Frequency Band

Javier Alvaro Rivera Suaña

June 2017

Master's Thesis in Electronics

Master's Program in Electronics/Telecommunications

Examiner: Daniel Rönnow

Supervisor: Ernesto Ávila Navarro

Acknowledgements

First of all, I would like to express my gratitude to Prof. Edvard Nordlander, Jose Chilo and Javier Mendoza, who have given me the opportunity to study this master's program in Sweden, and to have shared wonderful moments as a student with all staff at ITB/Electronics, University of Gävle.

I also want to express my special thanks to my Supervisor Dr. Ernesto Ávila Navarro for his support and guidance throughout this thesis period at the Radio-communications and Microwave Electronics department of the Miguel Hernandez University of Elche, UMH, Spain. Also, special thanks to Dr. Alberto Rodriguez and Hector Garcia.

I would also like to express my gratitude towards my examiner Prof. Daniel Rönnow at ITB/Electronics, University of Gävle, for valuable comments on the report.

To all my friends in Gävle, especially Guido, Salim and Sedat who have helped me to continue studying. I will never forget all those moments doing assignments in the laboratory.

Finally, I would like to show my thanks and appreciation to my loving parents in Perú for their infinite support given to me every day.

In memory of my cousin Fredy

Abstract

The purpose of this project was to design and manufacture a Low-Noise Amplifier (LNA) working at a 5 GHz frequency band, by using High Electron Mobility Transistor (HEMT) from Avago Technologies. To improve our design, it was necessary to build a two-stage amplifier; one stage to work in minimum noise sensitivity, and another stage to get the maximum gain achievable by the transistor. This thesis work was carried out as a part of the UAV (Unmanned Aerial Vehicle) system project developed by a research group at the Radio communication and Microwave Electronics department, UMH.

The project was designed and simulated using Agilent ADS (Advanced Design System) software.

Table of contents

Acknowledgements	i
Abstract	ii
Table of contents	iii
List of figures	vi
List of tables	viii
1 Introduction	1
1.1 Goal	1
1.2 Method	1
1.3 Outline.....	2
2 Theory	3
2.1 Frequency band	3
2.2 Microwave theory.....	3
2.2.1 Transmission lines.....	3
2.2.2 Microstrip transmission line.....	5
2.2.3 Quarter-wave transformer	6
2.3 Scattering parameters	7
2.4 Microwave transistor amplifier	8
2.4.1 Gain	8
2.4.2 Stability	9
2.4.3 Maximum gain (conjugate matching)	10
2.4.4 Low-noise.....	11
2.4.5 Cascaded noise figure.....	12
2.4.6 Gain compression.....	13
3 Design.....	14
3.1 Characterization of the substrate	14
3.1.1 Dielectric constant (ϵ_r)	14
3.1.2 Loss tangent ($\tan\delta$).....	16

3.2	Selection of the transistor	17
3.2.1	DC-bias point for the transistor	17
3.3	Selection of the DC-blocking capacitor	19
3.4	DC-bias circuit for the transistor	19
3.4.1	Design of microstrip radial resonator	20
3.4.2	Design of microstrip RF choke.....	21
3.5	Maximum-gain amplifier	22
3.5.1	Schematic design.....	22
3.5.2	EM-cosimulation design.....	27
3.6	Minimum-noise amplifier.....	28
3.6.1	Schematic design.....	28
3.6.2	EM-cosimulation design.....	32
3.7	Design of two-stage LNA.....	34
3.7.1	First stage	34
3.7.2	Second stage	34
3.7.3	Intermediate matching network.....	34
3.7.4	Design of matching networks for the cascaded LNA.....	35
3.7.5	EM-cosimulation for the cascaded LNA.....	38
4	Manufacturing	39
4.1	Insulator technique	39
5	Measurements.....	40
5.1	Measurements equipment.....	40
5.1.1	E8363B network analyzer	40
5.1.2	N4693A electronic calibration module	40
5.2	Maximum-gain amplifier	41
5.3	Minimum-noise amplifier.....	41
5.4	Minimum noise and maximum-gain amplifier.....	42
6	Discussion	44
7	Conclusions	48

References 49

Appendix A 1

List of figures

Fig. 1. Frequency band designation [1].	3
Fig. 2. General model for transmission line in short section Δz [6].	4
Fig. 3. Microstrip transmission line [1].	5
Fig. 4. Quarter-wave matching transformer [1].	7
Fig. 5. S-parameters representing for a two-port network [8].	7
Fig. 6. Transistor amplifier circuit [1].	9
Fig. 7. Cascade transistor amplifiers.	12
Fig. 8. Gain compression behavior.	13
Fig. 9. Quarter-wave resonator circuit.	14
Fig. 10. Resonance frequencies obtained from the quarter-wave circuit.	15
Fig. 11. Dielectric constants (ϵ_r) obtained after made the tuning.	15
Fig. 12. Characterization for the $\tan\delta$ of the substrate.	16
Fig. 13. Pin connections and recommended PCB pad Layout for the transistor.	17
Fig. 14. DC-bias circuit for the transistor ATF-34143.	18
Fig. 15. Simulated $I_{DS} - V_{DS}$ from the ATF-34143 transistor.	18
Fig. 16. Quarter-wave short circuit stub [11].	19
Fig. 17. The design circuit for the radial resonator.	20
Fig. 18. Impedance response from the radial resonator.	20
Fig. 19. RF-choke circuit.	21
Fig. 20. Results from the RF-Choke circuit.	22
Fig. 21. DC-bias network for the maximum-gain amplifier.	22
Fig. 22. Source and load stability circles.	23
Fig. 23. Conjugate reflection coefficients.	24
Fig. 24. Maximum-gain amplifier.	25
Fig. 25. Conjugate reflections Γ_L and Γ_S matched.	26
Fig. 26. S-Parameters from the maximum-gain amplifier.	26
Fig. 27. Layout generated for the maximum-gain amplifier.	27
Fig. 28. EM-cosimulation results from the maximum-gain amplifier.	27

Fig. 29. DC bias network for the minimum-noise amplifier..... 28

Fig. 30. Optimum and conjugate coefficients for the minimum-noise amplifier. 29

Fig. 31. Minimum-noise amplifier. 30

Fig. 32. Reflection coefficients matched for the minimum-noise amplifier. 31

Fig. 33. S-parameters results from the minimum-noise amplifier. 31

Fig. 34. Noise figure achieved from the amplifier. 32

Fig. 35. Layout for the minimum-noise amplifier. 32

Fig. 36. EM-cosimulation results from the minimum-noise amplifier. 33

Fig. 37. Intermediate matching coefficients for the cascaded LNA. 35

Fig. 38. Intermediate-matching network for the cascaded LNA. 35

Fig. 39. Cascaded LNA. 36

Fig. 40. Input and output coefficients matched. 36

Fig. 41. Schematic results from the cascaded LNA..... 37

Fig. 42. Minimum-noise achieved from the cascaded LNA..... 37

Fig. 43. Layout generated for the cascaded LNA..... 38

Fig. 44. EM-cosimulation results from the cascaded LNA. 38

Fig. 45. Transparency film printed with the amplifier design..... 39

Fig. 46. Programmable desktop reflow oven. 39

Fig. 47. Vector Network Analyzer E8363B..... 40

Fig. 48. Electronic calibration module N4693A..... 40

Fig. 49. Comparison between the EM-cosimulation results and VNA measurements. 41

Fig. 50. Comparison between the EM-cosimulation results and VNA measurements. 42

Fig. 51. VNA measurement of the two-stage amplifier. 43

List of tables

<i>Table 1. Parameters characterized for the substrate.</i>	<i>44</i>
<i>Table 2. S-parameters obtained from the maximum-gain amplifier.</i>	<i>45</i>
<i>Table 3. S-parameters obtained from the minimum-noise amplifier.</i>	<i>45</i>
<i>Table 4. S-parameters obtained from the two stage amplifiers.</i>	<i>46</i>
<i>Table 5. EM-cosimulation results from the cascaded amplifier.</i>	<i>46</i>

1 Introduction

Nowadays there are several applications using the term *microwave* that is used to describe electromagnetic waves with a wavelength ranging between 10 cm and 1 mm. thus, the corresponding frequency range is between 3 GHz and 300 GHz [1]. In more recent years *microwave* frequencies have also come into widespread use in communications systems, radar applications; since the propagations of *microwave* is effectively along line-of-sight paths [2].

In RADAR (Radio Detection and Ranging System) applications, generally, a Low-Noise Amplifier (LNA) is placed at the front-end of a radio receiver system, which the main function is to provide the first stage of amplification in the receiver, prior to the signal being down-converted [3].

Thus, the Low-Noise Amplifier is one of the most critical stages in a communications system that is widely used in several applications like UAV (Unmanned Aerial Vehicle). Where, the noise figure of the LNA has the greatest impact by any component on the overall receiver, regarding noise figure and receiver sensitivity, therefore, the two performance specifications of primary importance to determine for LNA quality are gain and noise figure [4].

1.1 Goal

The overall goal of this project is to design and manufacture a Low-Noise Amplifier (LNA) working in the 5 GHz frequency band, the circuit design is intended to get two-stage amplifiers; the first stage to work with minimum noise, and the second stage to get the maximum gain achievable by the transistor. The expected results for this LNA design is to achieve more than 20 dB gain with a noise figure that is less than 1 dB.

1.2 Method

The method to successfully achieve the purpose of this project is by applying the necessary literature information and using as the main tool, Agilent ADS (Advanced Design System) software, to design the low-noise amplifier, and also to perform the EM-cosimulation in order to obtain more accurate simulation results of our design.

1.3 Outline

The structure of this thesis is as follow:

- **Chapter 2:** Theory. Covers the necessary literature information needed to be applied, in our whole design system.
- **Chapter 3:** Design. Displays step by step the entire design and simulation performed to get our Low-Noise Amplifier design.
- **Chapter 4:** Manufacturing. Shows the process to make the amplifiers.
- **Chapter 5:** Measurements. Displays the characterizations of the amplifiers.
- **Chapter 6:** Discussion. Covers the discussion regarding the results obtained.
- **Chapter 7:** Conclusion. Summarizes the whole process and results obtained to give some recommendations and suggestions for the improvement of this kind of work.

2 Theory

2.1 Frequency band

Since the purpose of this project is to design an LNA to be used in a UAV (Unmanned Aerial Vehicle) application, also named as *Drone*, the frequency band used to design is under C-band. Thus, most microwave frequencies at the radar applications are narrowband (< 10 % bandwidth), but, the trend of it is toward increasing bandwidth (e.g., 25%) [5].

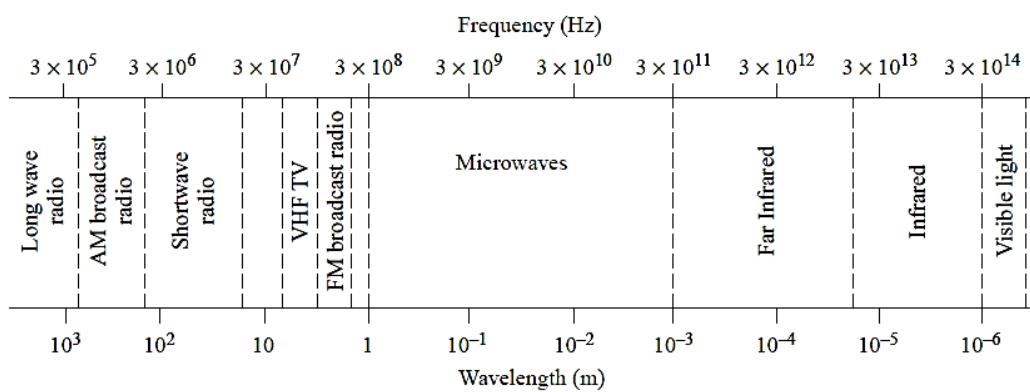


Fig. 1. Frequency band designation [1].

2.2 Microwave theory

2.2.1 Transmission lines

Working with high-frequency applications, there are three types of transmission lines: lossless transmission line, lossy transmission line and microstrip transmission line. Since the task of this project is on practical problem-solving, we will be focused on microstrip transmission line. However, it is important to consider the fundamental knowledge of transmission lines due to at high frequencies, transmission lines behave quite differently. For instance, short-circuits can actually have an infinite impedance; open-circuits can behave like short-circuited wires.

Thus, we can consider an equivalent circuit for a short section of transmission line, as shown in Fig. 2.

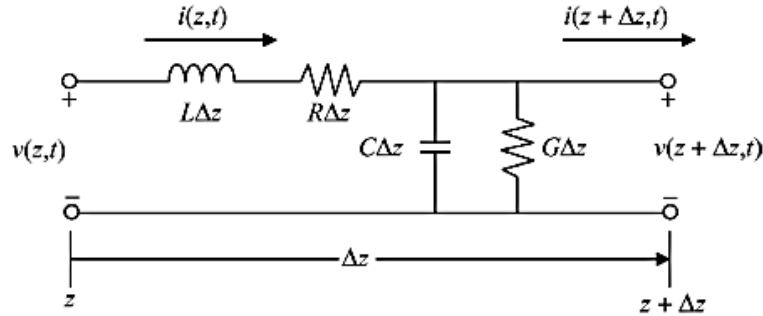


Fig. 2. General model for transmission line in short section Δz [6].

Where Δz is much smaller than a wavelength, the inductance and capacitance present in Fig. 2 provides the time delay and phase shift lacking in the treatment of these transmission lines using conventional circuit theory, therefore, it is available to analyze this equivalent lumped circuit by using Kirchoff's voltage and current laws. And, the quantity $L\Delta z$ (H) is the total series inductance of the equivalent circuit, which depends on the inductance per unit length L (H/m). $C\Delta z$ (F) is the total capacitance, which depends on the shunt capacitance per unit length C (F/m). The total series resistance $R\Delta z$ and shunt conductance $G\Delta z$ depend on the resistance per unit length R (Ω /m) and the conductance per unit length G (S/m), respectively.

The application of Kirchoff's voltage law to the equivalent circuit in Fig. 2 gives

$$v(z + \Delta z, t) + L\Delta z \frac{\partial i}{\partial t} + R\Delta z i(z, t) = v(z, t) \tag{1}$$

Which can be

$$\frac{v(z+\Delta z,t)-v(z,t)}{\Delta z} = -Ri(z, t) - L \frac{\partial i}{\partial t} \tag{2}$$

In the limiting case, as Δz tends to zero, this equation becomes

$$\frac{\partial v}{\partial z} = -Ri(z, t) - L \frac{\partial i}{\partial t} \tag{3}$$

And, the applications of Kirchhoff's current law to the circuit in Fig. 2 produces

$$i(z + \Delta z, t) - i(z, t) = -G\Delta z v(z + \Delta z, t) - C\Delta z \frac{\partial v}{\partial t} \quad (4)$$

Which, in the limiting case as $\Delta z \rightarrow 0$, gives

$$\frac{\partial i}{\partial z} = -Gv(z, t) - C \frac{\partial v}{\partial t} \quad (5)$$

where, equations (3) and (5) are known as *the transmission line equations* [6].

2.2.2 Microstrip transmission line

Nowadays, the microstrip transmission line provides a useful technique to a trace a PWB (Printed Wiring Board), where the signal consists of electric and magnetic fields between the conductor, which in actuality fringe around the conductor edges, as shown in Fig. 3.

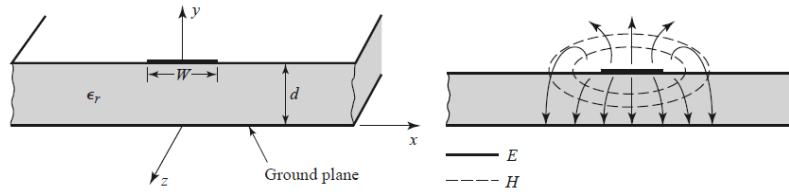


Fig. 3. Microstrip transmission line [1].

The *effective dielectric constant* (ϵ_e) of the microstrip line is in the dielectric region and some in air, thus, the *effective dielectric constants* (ϵ_e) should satisfy the relation

$$1 < \epsilon_e < \epsilon_r$$

Where the effective dielectric constant of a microstrip line is given by

$$\epsilon_e = \frac{\epsilon_r + 1}{2} + \frac{\epsilon_r - 1}{2} \frac{1}{\sqrt{1 + 12 \frac{d}{W}}} \quad (6)$$

And, given the dimension of the microstrip line, the characteristic impedance can be calculated as follow

For $\frac{W}{d} \leq 1$

$$Z_0 = \frac{60}{\sqrt{\epsilon_e}} \ln \left(\frac{8d}{W} + \frac{W}{4d} \right) \quad (7)$$

For $\frac{W}{d} \geq 1$

$$Z_0 = \frac{120\pi}{\sqrt{\epsilon_e} \left[\frac{W}{d} + 1.393 + 0.667 \ln \left(\frac{W}{d} + 1.444 \right) \right]} \quad (8)$$

Nevertheless, for a given *characteristic impedance* (Z_0) and *dielectric constant* (ϵ_r), the W/d ratio can be calculated as

For $\frac{W}{d} < 2$

$$\frac{W}{d} = \frac{8e^A}{e^{2A}-2} \quad (9)$$

For $\frac{W}{d} > 2$

$$\frac{W}{d} = \frac{2}{\pi} \left[B - 1 - \ln(2B - 1) + \frac{\epsilon_r - 1}{2\epsilon_r} \left\{ \ln(B - 1) + 0.39 - \frac{0.61}{\epsilon_r} \right\} \right] \quad (10)$$

Where

$$A = \frac{Z_0}{60} \sqrt{\frac{\epsilon_r + 1}{2}} + \frac{\epsilon_r - 1}{\epsilon_r + 1} \left(0.23 + \frac{0.11}{\epsilon_r} \right) \quad (11)$$

$$B = \frac{377\pi}{2Z_0\sqrt{\epsilon_r}} \quad (12)$$

2.2.3 Quarter-wave transformer

One of the most common intermediate circuit for impedance matching is the quarter-wave transformer, which implies a transmission line. Thus, the input impedance of the right-hand transmission line shown in Fig.4. is given by Eq. (13).

$$Z_{in} = Z_1 \frac{R_L + jZ_1 \tan \beta \ell}{Z_1 + jR_L \tan \beta \ell} \quad (13)$$

And to evaluate $\ell = \lambda/4$ in Eq. 13, we have $\beta\ell = (2\pi/\lambda)/(\lambda/4) = \pi/2$, and dividing the numerator and denominator by $\beta\ell$, also taking the limit as $\beta\ell$ tends to $\pi/2$, it gives

$$Z_{in} = Z_1^2 / Z_L \tag{14}$$

Thus, in order to get $\Gamma = 0$, we must have $Z_{in} = Z_0$, which gives the characteristic impedance of the quarter-wave transformer

$$Z_1 = \sqrt{Z_0 R_L} \tag{15}$$

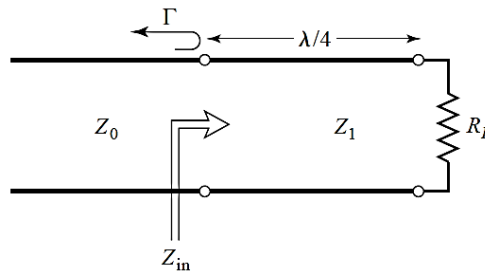


Fig. 4. Quarter-wave matching transformer [1].

2.3 Scattering parameters

Scattering parameters are one of the most useful tools to see the overall behavior of an N-port network when is necessary to measure all reflection coefficients at microwave frequencies given by S-parameters. Also, dealing a direct measurement of impedance, admittance or *ABCD* parameters require that the ports should be terminated in either short or open circuit. Thus, the essence of scattering parameters is that they relate forward and backward-traveling waves (power flow) on a transmission line [7].

The S-Parameters of two-port circuits is characterized by four parameters as shown in Fig.5.

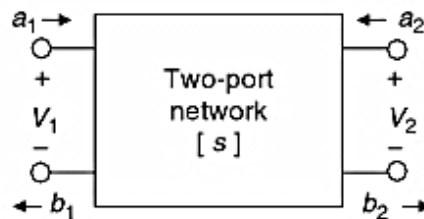


Fig. 5. S-parameters representing for a two-port network [8].

From the figure above the S-parameters can be represented by the relationship between a_n and b_n as follow [8].

$$a_n = \frac{v_n^+}{\sqrt{Z_{0n}}} \quad ; \text{ Proportional to the incoming wave at the } n^{\text{th}} \text{ port}$$

$$b_n = \frac{v_n^-}{\sqrt{Z_{0n}}} \quad ; \text{ Proportional to the outgoing wave at the } n^{\text{th}} \text{ port}$$

Where v_n^+ and v_n^- represent voltages corresponding to the incoming and the outgoing waves in the transmission line connected to the n^{th} port and Z_{0n} (characteristic impedance) of the line; thus, the relationship between a_n and b_n can be written as

$$b_1 = S_{11}a_1 + S_{12}a_2$$

$$b_2 = S_{21}a_1 + S_{22}a_2$$

Therefore, we have

$$S_{11} = \frac{b_1}{a_1}, \quad S_{21} = \frac{b_2}{a_1}, \quad a_2 = 0$$

$$S_{12} = \frac{b_1}{a_2}, \quad S_{22} = \frac{b_2}{a_2}, \quad a_1 = 0$$

Where

S_{11} = Input reflection coefficient

S_{21} = Forward transmission coefficient

S_{12} = Reverse transmission coefficient

S_{22} = Output reflection coefficient

2.4 Microwave transistor amplifier

2.4.1 Gain

Since voltage and current are extremely difficult to measure at high frequencies, it is much easier to measure signal power. At the same time, the interstage impedance levels achievable at high frequencies are neither very high nor very small, making power, rather than voltage gain or current gain, critically important in high-frequency circuit design.

We will consider an arbitrary two-port network, characterized by its S-parameters connected to the source and load impedance Z_S and Z_L , respectively, as shown in Fig. 6 to define the power gains acting on the two-port network.

- *The power gain, $G = P_L/P_{in}$* is defined as the power dissipated in the load divided by the power delivered to the input of the two-port network. It is independent of the signal source impedance Z_S .
- *The available power gain, $G_A = P_{avn}/P_{avs}$* is defined as the power available from the two-port network divided by the power available from the signal source. It assumes conjugate matching of the source and of the load, thus, it is dependent on the signal source impedance, but not on the load impedance Z_L .
- *Transducer power gain, $G_T = P_L/P_{avs}$* is one the most useful figures for an amplifier, which is the ratio of the power delivered to the load of the power delivered by the source and it depends on the input and output match. Thus, in terms of the gain coefficients, the transducer gain is $G_T = G_S G_0 G_L$. And in terms of reflection coefficients, the transducer gain is given as:

$$G_T = \frac{1 - |\Gamma_S|^2}{|1 - \Gamma_{in} \Gamma_S|^2} |S_{21}|^2 \frac{1 - |\Gamma_L|^2}{|1 - S_{22} \Gamma_L|^2}$$

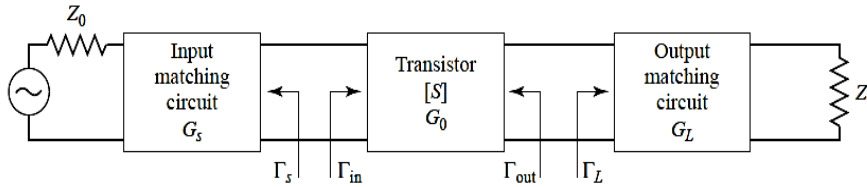


Fig. 6. Transistor amplifier circuit [1].

2.4.2 Stability

The stability is a necessary condition for a transistor amplifier to guarantee the right performance of an LNA design in a stable region. Thus, there are two types of stability:

$$|\Gamma_{in}| = \left| S_{11} + \frac{S_{12} S_{21} \Gamma_L}{1 - S_{22} \Gamma_L} \right| < 1$$

$$|\Gamma_{out}| = \left| S_{22} + \frac{S_{12} S_{21} \Gamma_S}{1 - S_{11} \Gamma_S} \right| < 1$$

- Unconditional stability, where the input and output reflection coefficients are

$$|\Gamma_{in}| < 1 \text{ and } |\Gamma_{out}| < 1$$

For all passive source and load impedances.

- Conditional stability, where the input and output reflection coefficient are

$$|\Gamma_{in}| < 1 \text{ and } |\Gamma_{out}| < 1$$

Only for a certain range of passive source and load impedances.

Thus, the stability is needed before to make the design of an amplifier and can determine the stability region for Γ_S and Γ_L . To analyze this stability condition, it can be determined by using the *Rollet's condition* as defined below

$$K = \frac{1 - |S_{11}|^2 - |S_{22}|^2 + |\Delta|^2}{2|S_{12}S_{21}|} > 1$$

Where

$$|\Delta| = |S_{11}S_{22} - S_{12}S_{21}| < 1$$

2.4.3 Maximum gain (conjugate matching)

To get the maximum gain between the *Source* and *Load* impedances of the transistor, it must be realized when the *Source* and *Load* reflection coefficients provide a conjugate matching on them. Thus, the maximum power transfer from the input matching network to the transistor will occur when

$$\Gamma_{in} = \Gamma_S^*$$

And the maximum power transfer from the transistor to the output matching network will occur when

$$\Gamma_{out} = \Gamma_L^*$$

With those assumptions for lossless matching networks, the overall transducer gain for maximum gain will be given by

$$G_{Tmax} = \frac{1}{1 - |\Gamma_S|^2} |S_{21}|^2 \frac{1 - |\Gamma_L|^2}{|1 - S_{22}\Gamma_L|^2}$$

And, the necessary equations to get the maximum gain in a bilateral case is as follow

$$\Gamma_S^* = S_{11} + \frac{S_{12}S_{21}\Gamma_L}{1 - S_{22}\Gamma_L}$$

$$\Gamma_L^* = S_{22} + \frac{S_{12}S_{21}\Gamma_S}{1 - S_{11}\Gamma_S}$$

Where the solution of Γ_S and Γ_L are given as

$$\Gamma_S = \frac{B_1 \pm \sqrt{B_1^2 - 4|C_1|^2}}{2C_1}$$

$$\Gamma_L = \frac{B_2 \pm \sqrt{B_2^2 - 4|C_2|^2}}{2C_2}$$

The variables B_1 , C_1 , B_2 , C_2 are defined as

$$B_1 = 1 + |S_{11}|^2 - |S_{22}|^2 - |\Delta|^2$$

$$B_2 = 1 + |S_{22}|^2 - |S_{11}|^2 - |\Delta|^2$$

$$C_1 = S_{11} - \Delta S_{22}^*$$

$$C_2 = S_{22} - \Delta S_{11}^*$$

2.4.4 Low-noise

The noise figure of a two-port amplifier can be expressed as

$$F = F_{min} + \frac{R_N}{G_S} |Y_S - Y_{opt}|^2$$

Where

Y_S = Source admittance presented to transistor.

Y_{opt} = Optimum source admittance to get minimum noise figure.

F_{min} = Minimum noise figure of transistor

R_N = Equivalent noise resistance of transistor.

G_S = Real part of source admittance.

Thus, in order to achieve the minimum noise in a LNA design, it must be applied that

$$Y_s = Y_{opt}$$

2.4.5 Cascaded noise figure

Noise figure is one of the most important parameters, when we are designing a Low-noise amplifier, especially in cascaded amplifiers, where the cumulative noise figure of two or more cascaded amplifiers is described by Eq. (16), which is defined as *Friis's equation* [9].

Fig. 7. shows the gain and noise figure of the individual stages of a cascade transistor amplifier.

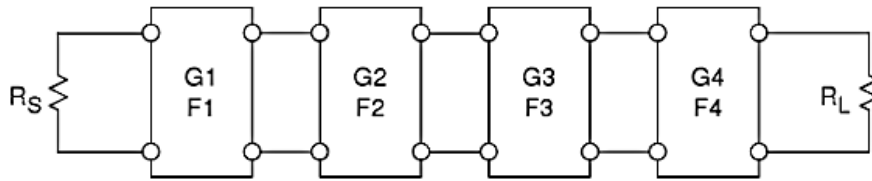


Fig. 7. Cascade transistor amplifiers.

$$F_{total} = F_1 + \frac{F_2-1}{G_1} + \frac{F_3-1}{G_1G_2} + \dots + \frac{F_n-1}{G_1G_2G_3\dots G_n} \tag{16}$$

Where:

F_{total} = Noise figure of the amplifiers cascaded together

F_n = Noise figure of the n^{th} amplifier

G_n = Gain of the n^{th} amplifier

Thus, in a cascade amplifier, the final stage sees an input signal that consists of the original signal and noise amplified by each successive stage. Each stage in the cascade chain amplifies signal and noise from previous stages and contributes some noise of its own. As we can see in Eq. (16). the noise figure of the entire cascade chain is dominated by the noise contribution of the first stage or two; later stages are less important where noise is concerned, provided that the input stages have sufficient gain.

2.4.6 Gain compression

Gain compression is a usual behavior of a typical microwave amplifier, especially, when we are plotting the output power as a function of input power. At low power levels, a single frequency signal is increased in power level by the small signal gain, as $P_{out} = G * P_{in}$, where at lower power levels, this produces a linear P_{out} versus P_{in} plot with slope equals one.

At higher levels, nonlinearities in the amplifier begin to generate some power in the harmonics of the single frequency input signal and to compress the output signal. Therefore, gain compression is often characterized in terms of the power level when the large signal gain is 1 dB less than the small gain, as shown in Fig. 8.

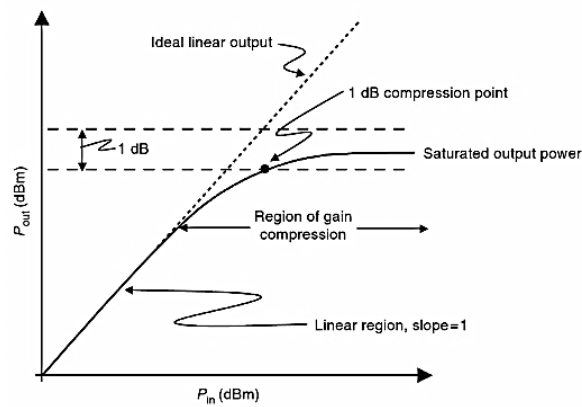


Fig. 8. Gain compression behavior.

3 Design

3.1 Characterization of the substrate

3.1.1 Dielectric constant (ϵ_r)

The purpose of this characterization is to find the most accurate value of the dielectric constant (ϵ_r) of the substrate used, which is correlated with the design frequency. The task will be designing and manufacturing a resonator circuit at 2.5 GHz, to later on, make it an adjustment with the schematic and momentum simulations, in order to do an average of those values of the dielectric constant.

To carry out this resonator design, we will take the parameters of the substrate given by the manufacturer.

- $\epsilon_r = 4.4$; Dielectric constant
- $H = 0.4 \text{ mm}$; Thickness of the substrate
- $\tan \delta = 0.02$; Loss tangent
- $T = 35 \mu\text{m}$; Thickness of the conductor

As we can see in Fig. 9. The quarter-wave resonator has been designed at 2.5 GHz.

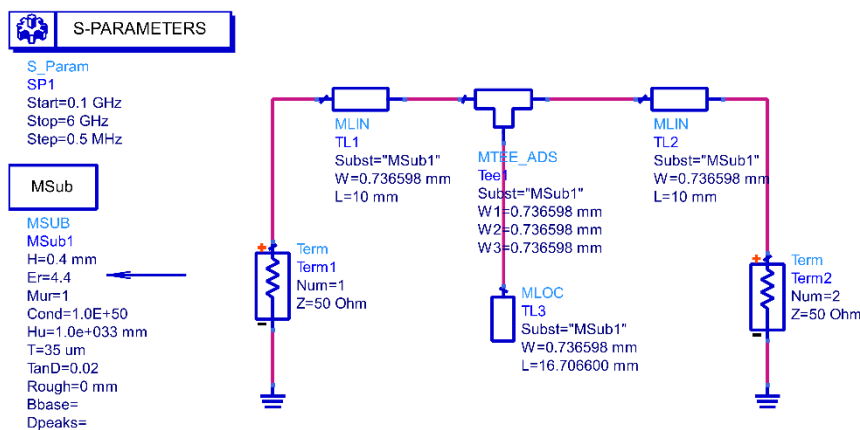


Fig. 9. Quarter-wave resonator circuit.

Once we have designed the resonator circuit, we proceed to measure it, where, we got different frequencies from the schematic simulation at 2.499 GHz and momentum simulation at 2.477 GHz, while VNA measurement at 2.544 GHz. As shown in Fig. 10.

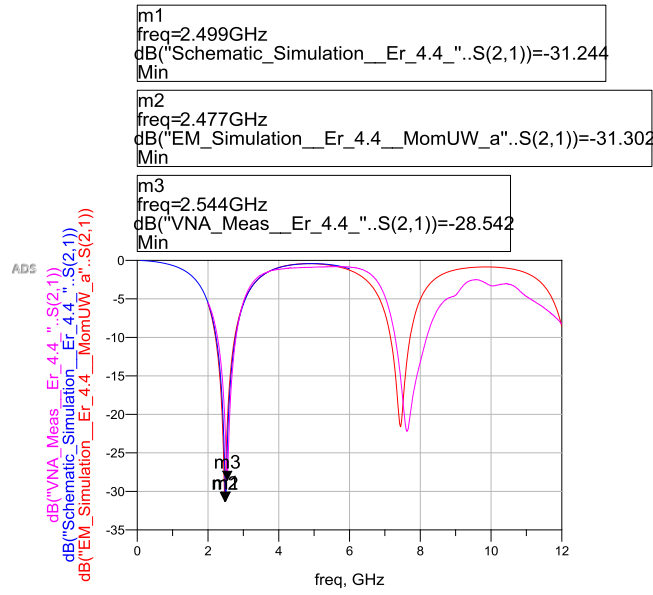


Fig. 10. Resonance frequencies obtained from the quarter-wave circuit.

Then, due to the different resonance frequencies obtained, the task was to do a tuning on the dielectric parameter of the schematic and momentum design, in order to get the same frequency as VNA measurement at 2.544 GHz. After doing that process, we got the dielectric constants; from the schematic simulation at 4.23 and momentum simulation at 4.19, which are different from each other. As shown in Fig. 11.

Thus, the dielectric constant taken to design the amplifiers was $\epsilon_r = 4.21$, which was obtained as an average of the schematic and momentum values.

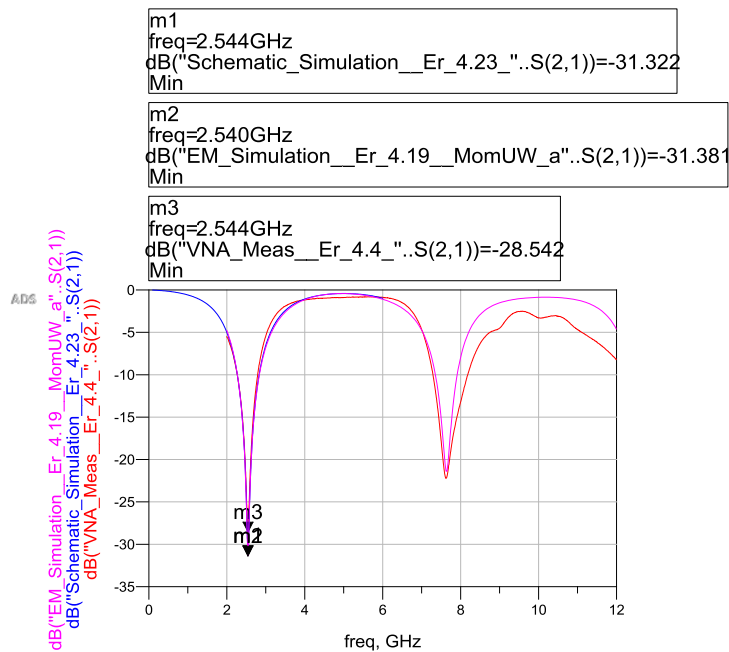


Fig. 11. Dielectric constants (ϵ_r) obtained after made the tuning.

3.1.2 Loss tangent ($\tan \delta$)

For this purpose, we will take as a reference the reflection coefficient S_{11} measured by VNA at the resonance frequency obtained (2.544 GHz) to make a *tuning* on the schematic design circuit from the Fig. 9.

As we can see in Fig. 12 (left side), it shows S_{11} (schematic simulation) compared to the VNA measurement result, both responses with $\tan \delta$ equals 0.02, but, we can see on it that the VNA attenuation result is more than the schematic attenuation result. Thus, we did a *tuning* on $\tan \delta$ from the schematic design, in order to achieve almost the same attenuation as the VNA result, as we can see in Fig. 12 (right side), the tuning on $\tan \delta$ parameter for the Schematic design is giving 0.042.

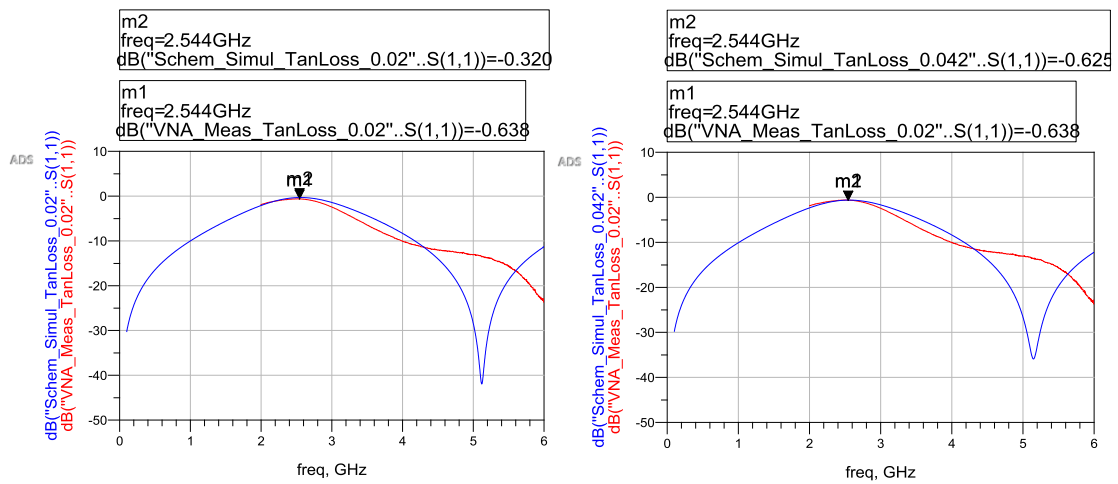


Fig. 12. Characterization for the $\tan \delta$ of the substrate.

3.2 Selection of the transistor

Since our LNA design will work at 5 GHz, and in order to achieve the minimum noise at the first stage of the amplifier and the maximum gain at the second stage of it; High Electron Mobility Transistor HEMT (ATF-34143) by AVAGO Technology is ideal for this type of requirements due to its excellent combination of low noise performance for a wider frequency range, high gain and high output power [10].

Also as a recommendation from the manufacturer, we will design the recommended PCB Pad Layout dimensions for this transistor given on data sheet, as shown in Fig. 13.

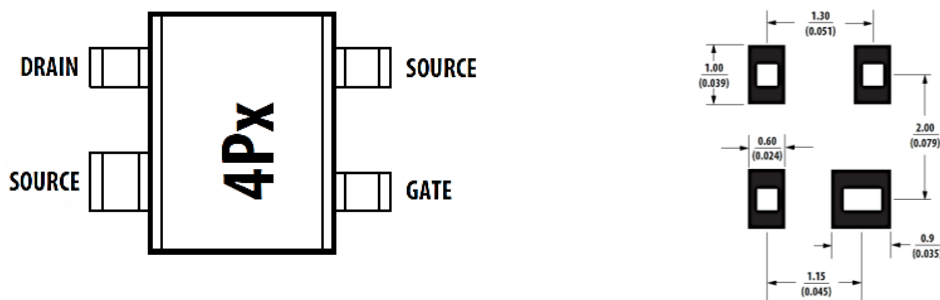


Fig. 13. Pin connections and recommended PCB pad Layout for the transistor.

3.2.1 DC-bias point for the transistor

In order to get the right performance of the transistor (ATF-34143), we will choose a proper DC-bias point for it. And by checking the available Drain-Source Voltage (V_{DS}) and Drain-Source Current (I_{DS}) for different scattering parameters given on data sheet, as follow

$$V_{DS} = 3V, I_{DS} = 20 \text{ mA}$$

$$V_{DS} = 3V, I_{DS} = 40 \text{ mA}$$

$$V_{DS} = 4V, I_{DS} = 40 \text{ mA}$$

$$V_{DS} = 4V, I_{DS} = 60 \text{ mA}$$

Where, it was necessary to apply the condition for unconditional stability on S-parameters for $V_{DS} = 4V$ and $I_{DS} = 40 \text{ mA}$, the Rollet's factor (K) was more than one at the design frequency of 5 GHz. Thus, we chose $V_{DS} = 4V$ and $I_{DS} = 40 \text{ mA}$ as DC- bias point for the transistor.

Fig. 14. shows the circuit for the transistor to find the proper DC-bias point of the voltage Gate-Source (V_{GS}).

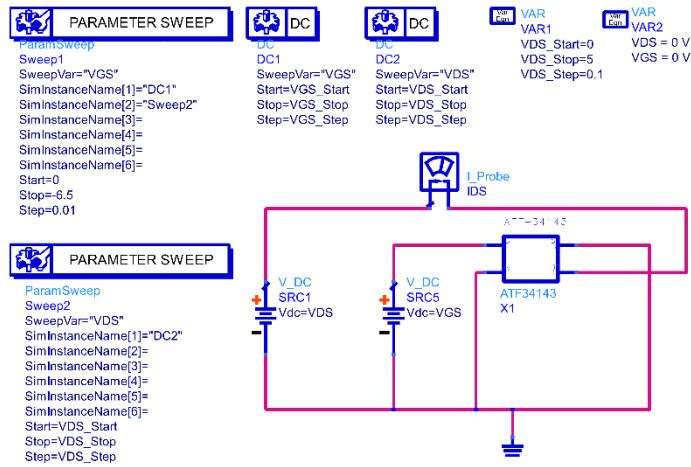


Fig. 14. DC-bias circuit for the transistor ATF-34143.

After doing the simulation of the DC-bias circuit to get the proper Voltage Gate-Source (V_{GS}) of the transistor, we got -0.54 V as the proper value. As shown in Fig. 15.

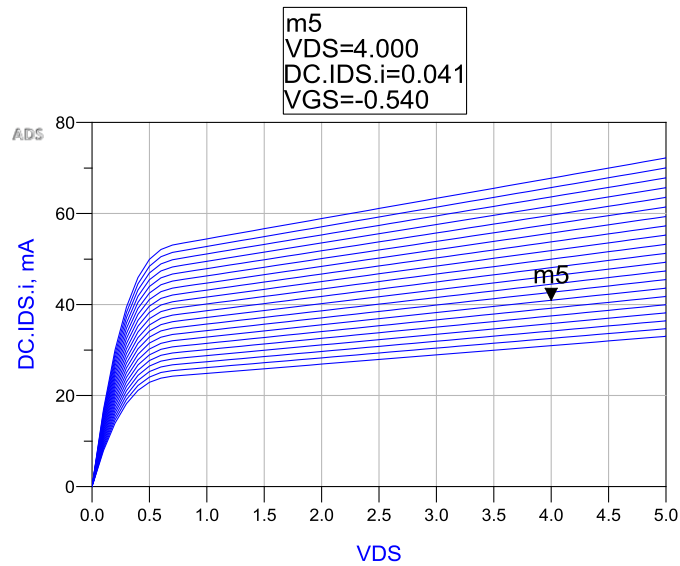


Fig. 15. Simulated $I_{DS} - V_{DS}$ from the ATF-34143 transistor.

3.3 Selection of the DC-blocking capacitor

In order to get a proper capacitor for DC blocking and coupling, it is necessary to consider typical requirements like capacitance, tolerance and voltage rating at the design frequency. Thus, there is a suitable capacitor model TDK (multilayer ceramic chip capacitor) to covers all these requirements. The 100 nF capacitor will be used in this project, with (TDK_C1608X8R1E104K080AA) taken as a reference model.

3.4 DC-bias circuit for the transistor

To perform the DC-bias circuit for the transistor amplifier, it is convenient to use a quarter-wave transmission line at the fundamental frequency to be able to do the connection between the *Drain* of the transistor and the DC-supply, similarly for the *Gate* of the transistor. This quarter-wave has the advantage of being as an open circuit at the fundamental frequency [11]. This advantage is important in order to avoid that the RF-signal goes to the DC-supply, also to strengthen this design at the end of the quarter-wave, we will be placed a radial resonator stub to guarantee a short-circuit.

As we can see in Fig. 16. An example of a circuit to place the quarter-wave transformer as a part of the DC-bias network for the transistor.

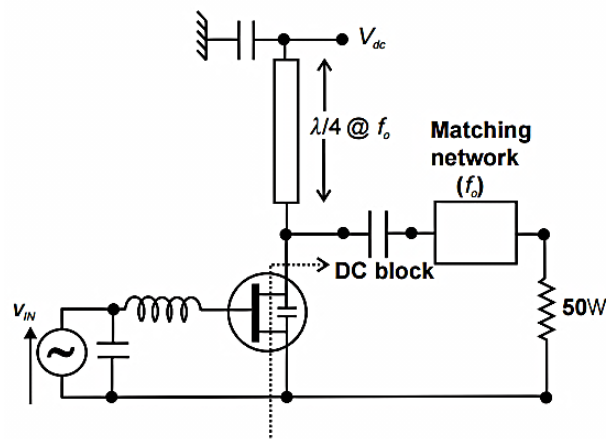


Fig. 16. Quarter-wave short circuit stub [11].

3.4.1 Design of microstrip radial resonator

Since this radial resonator needs to generate an RF-short circuit at the end of the quarter-wave transformer. Thus, it will be designed to work at 5 GHz and to achieve this requirement, this radial will depend on three dimensions like its width, length, and angle. As shown in Fig. 17.

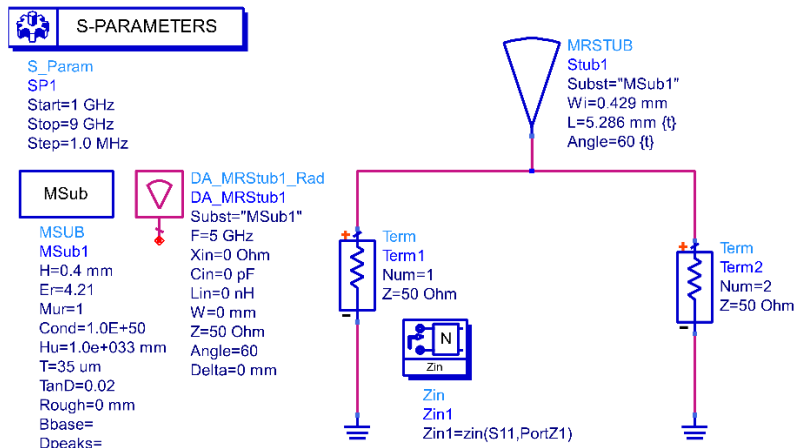


Fig. 17. The design circuit for the radial resonator.

As we can see in Fig. 18 the impedance obtained from the simulation of the radial circuit is -68.558 dB.

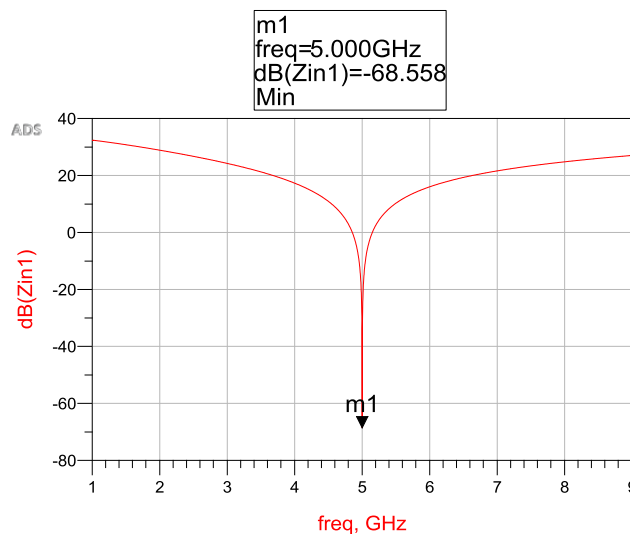


Fig. 18. Impedance response from the radial resonator.

3.4.2 Design of microstrip RF choke

Working at high frequencies, it is necessary to use an RF-choke circuit that is used to suppress the AC signals while passing the DC signal. Ideally, it is an inductor with infinite inductance value and low resistance [12].

To perform this RF-choke circuit for biasing the transistor, it is suitable to add a small transmission line (*MTaper*) to link the *Gate* and *Drain* paths of the transistor, in order to have more flexibility at the time when we will make the manufacture of the amplifier, and also to consider into RF-choke circuit. Therefore, to be able to connect the *Gate* and *Drain* paths of the transistor to the DC-supply, this RF choke is used for this purpose by using quarter-wave transformer between those terminals of the transistor and the DC supply. The quarter-wave transformer is designed to work at high impedance with 0.4 mm of width to achieve an open circuit while the RF-signal will go throughout the RF-signal path; then at the end of this quarter-wave transmission line will be placed the radial resonator. Also, we added two transmission lines to be able to connect the DC-supply for the transistor, as shown in Fig. 19.

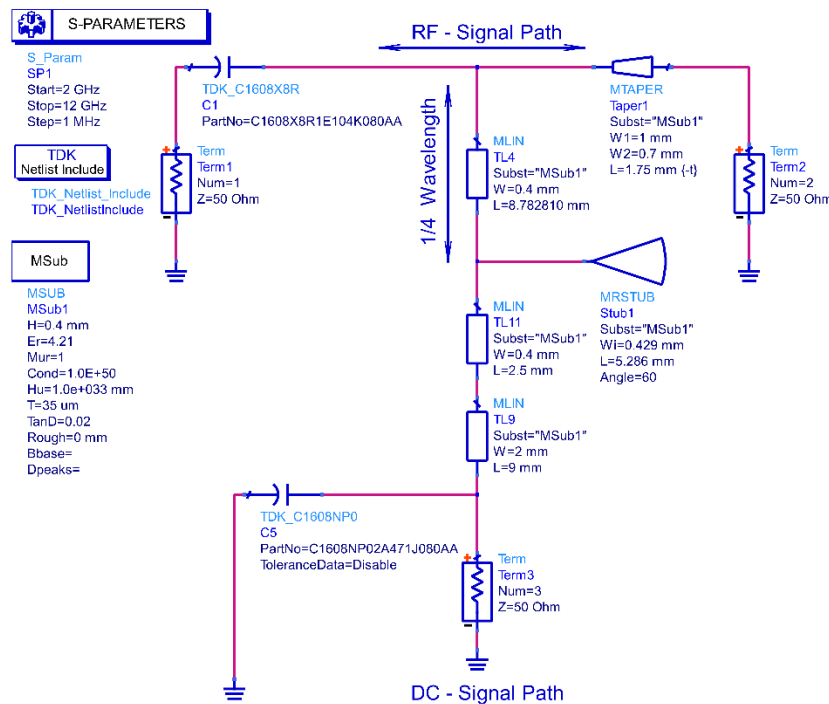


Fig. 19. RF-choke circuit.

Fig. 20 shows the results of this RF-choke circuit, where the forward transmission coefficient (S_{21}) is getting an attenuation of -0.132 dB for the RF-signal path, while the transmission (S_{31})

gets an attenuation of -99.796 dB, which means if the RF-signal could reach this point, it will act as a virtual ground or short-circuited.

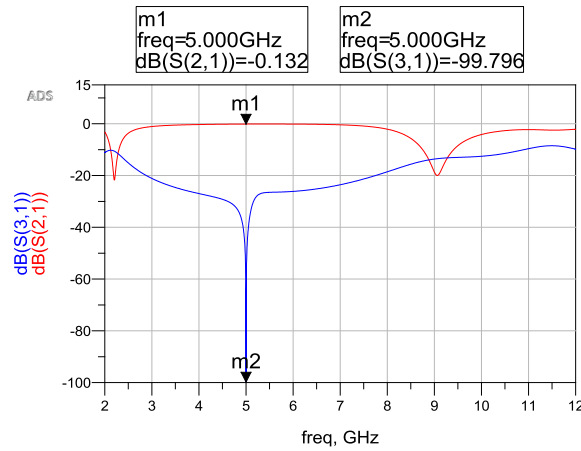


Fig. 20. Results from the RF-Choke circuit.

3.5 Maximum-gain amplifier

3.5.1 Schematic design

Since we have the RF-choke circuit for the transistor. We will design the maximum-gain amplifier by using the DC-bias network shown in Fig. 21. Also, we will use the S2P file to simulate the transistor. But, we must first check the stability of the DC-bias network.

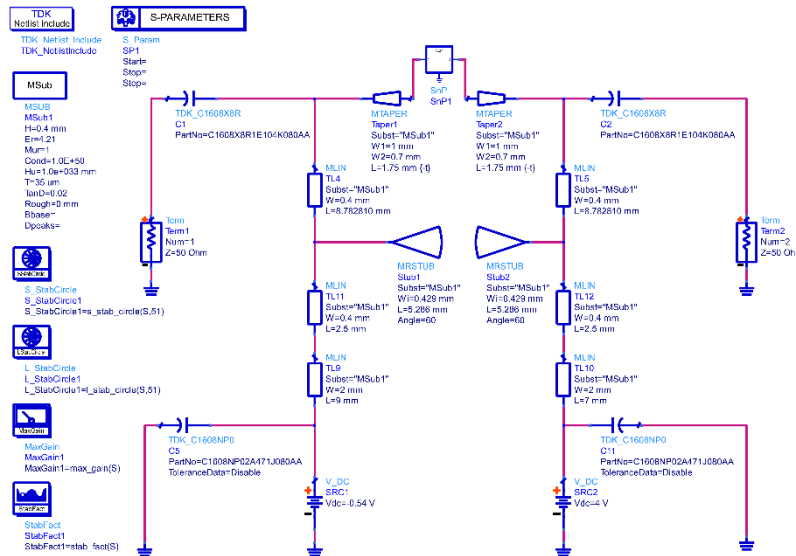


Fig. 21. DC-bias network for the maximum-gain amplifier.

After doing the simulation of the DC-bias network, we obtained the stability factor, which is given by *Rollet's condition* (k) that is more than one (1.063), meaning also that the DC-bias network is unconditionally stable to guarantee that both input and output reflection coefficients must be less than one ($|\Gamma_{in}| < 1, |\Gamma_{out}| < 1$) as well.

And, as we can see in Fig. 22. The source and load stability circles are outside of the Smith chart, where we can assume that inside of the Smith chart is unconditionally stable region by applying the requirements below

$$|\Gamma_{in}| = \left| S_{11} + \frac{S_{12}S_{21}\Gamma_L}{1 - S_{22}\Gamma_L} \right| < 1$$

$$|\Gamma_{out}| = \left| S_{22} + \frac{S_{12}S_{21}\Gamma_S}{1 - S_{11}\Gamma_S} \right| < 1$$

Thus, we must satisfy that Γ_L and Γ_S should be zero, regarding having $|\Gamma_{in}|=S_{11}$ and $|\Gamma_{out}|=S_{22}$ into above requirements. Therefore, we just need to analyze the absolute value of S_{11} and S_{22} , where both reflection coefficients are giving less than one, which are satisfying the above requirements, also, they are representing that the whole region inside of the Smith chart is unconditionally stable.

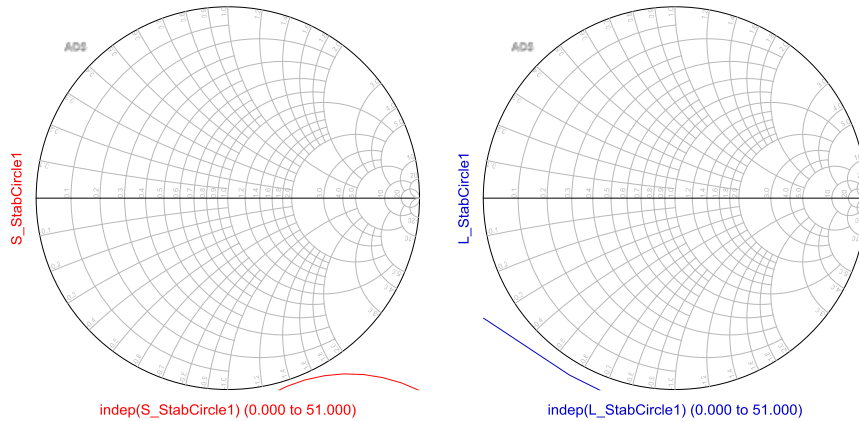


Fig. 22. Source and load stability circles.

S-parameters obtained from the simulation of the DC-bias network are given as follow

freq	S(1,1)	S(1,2)	S(2,1)	S(2,2)
5.000 GHz	0.680 / 62.677	0.105 / -77.153	2.616 / -56.153	0.296 / 65.055

Since the stability of the DC-bias network has been analyzed and the stable regions for *Source* and *Load* have been located on the Smith chart,

We need to find the necessary reflection coefficients at the input and output of the DC-bias network to get the maximum gain achievable by the transistor, where we must apply the conjugate matching on the DC-bias network by applying the necessary equations given in Subsection 2.4.3, where $\Gamma_{in} = \Gamma_S^*$ and $\Gamma_{out} = \Gamma_L^*$, as shown in Fig. 23.

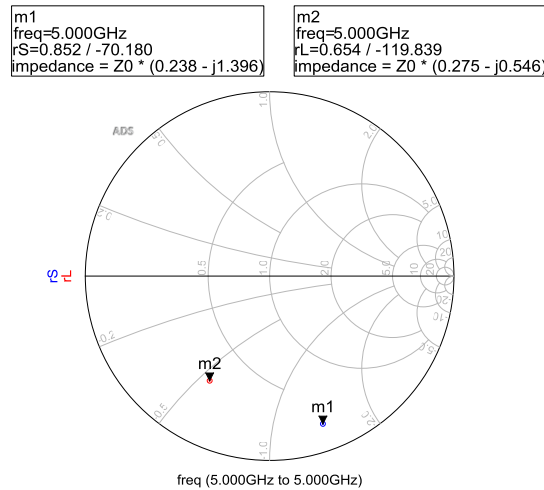


Fig. 23. Conjugate reflection coefficients.

Then, we can do the matching networks for the input and output of the DC-bias network by taking up the conjugate reflection coefficients given by Γ_L and Γ_S , and place them in the center of the Smith chart. ADS provide us an essential tool for this purpose that is *SmithChart*, where at the same time it can generate ideal transmission lines with *effective dielectric constants* (ϵ_e) at the characteristic impedance (50Ω). And, to be able to have these matching networks in microstrip lines, they must be converted as length (mm) and width (mm) by using *Linecal* tools.

Then, to be able to connect the SMA terminals to the ports for the amplifier, we must add characteristic transmission lines for the input and output. Also, it is better to add the *MTEE* junction between the matching networks and the characteristic transmission lines for the ports. After placing all these components on the design amplifier, it is convenient to do an adjustment onto lengths of the matching networks to make sure that both conjugate coefficients Γ_L and Γ_S are placed in the center of the Smith chart.

Thus, placing both conjugate coefficients in the center of the Smith chart, the overall transducer power gain of the amplifier will be controlled by the *Source* and *Load* gains of the matching networks.

Fig. 24 shows the full design for the amplifier to get the maximum gain by the transistor.

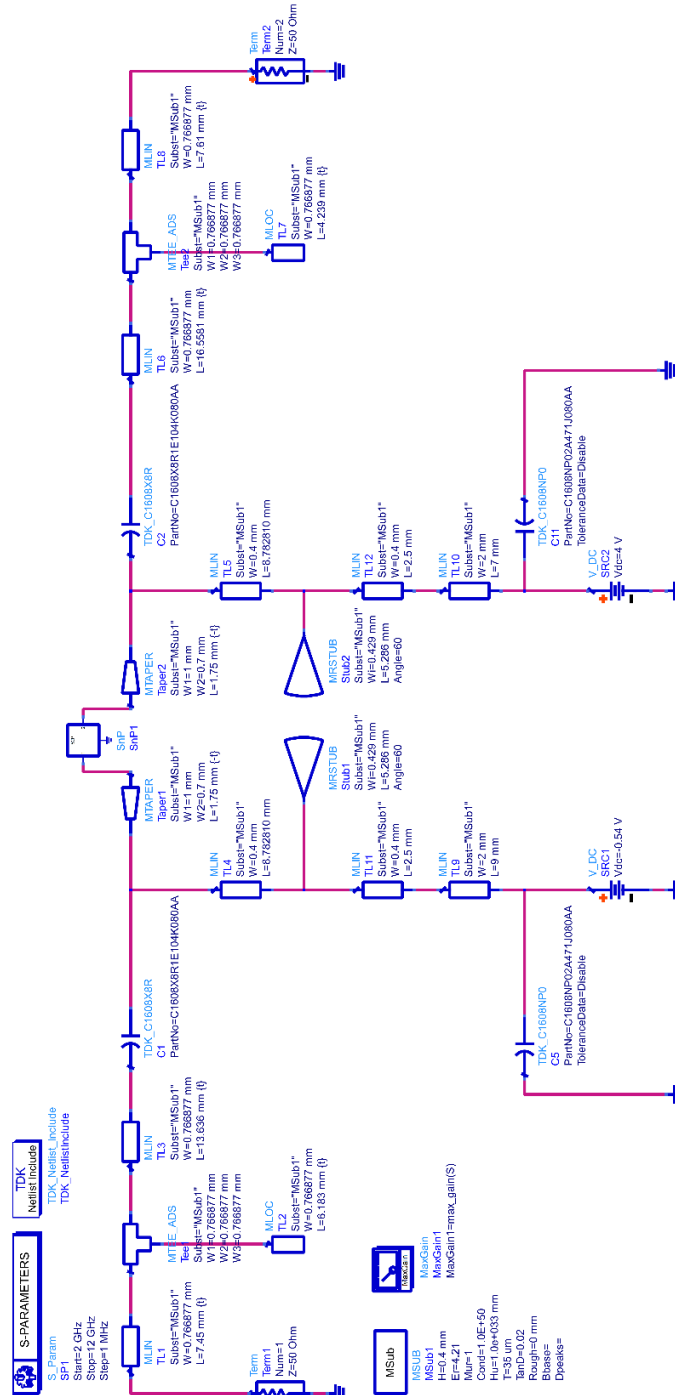


Fig. 24. Maximum-gain amplifier.

Since we have fixed the conjugate matching networks for the amplifier, and after doing the simulation of it. We can notice that both conjugate coefficients Γ_L and Γ_S are placed in the center of the Smith chart. As shown in Fig. 25.

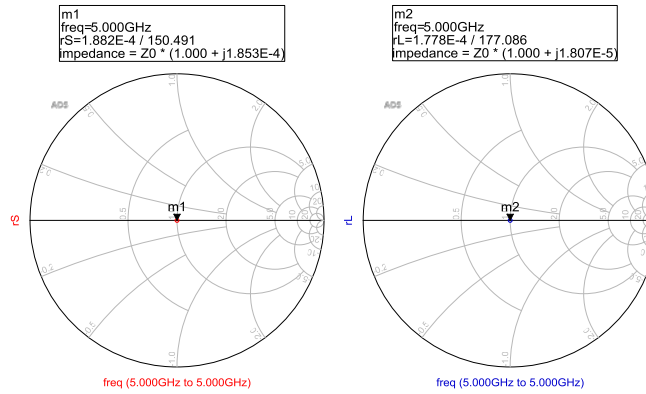


Fig. 25. Conjugate reflections Γ_L and Γ_S matched.

Fig. 26 shows the S-parameters from the simulation of the maximum-gain amplifier. Thus, the maximum gain provided by the amplifier is 10.409 dB, where the forward coefficient S_{21} reaches that maximum gain due to the conjugate matching. Also, we can see that both reflection coefficients S_{11} and S_{22} are matching the amplifier at the fundamental frequency.

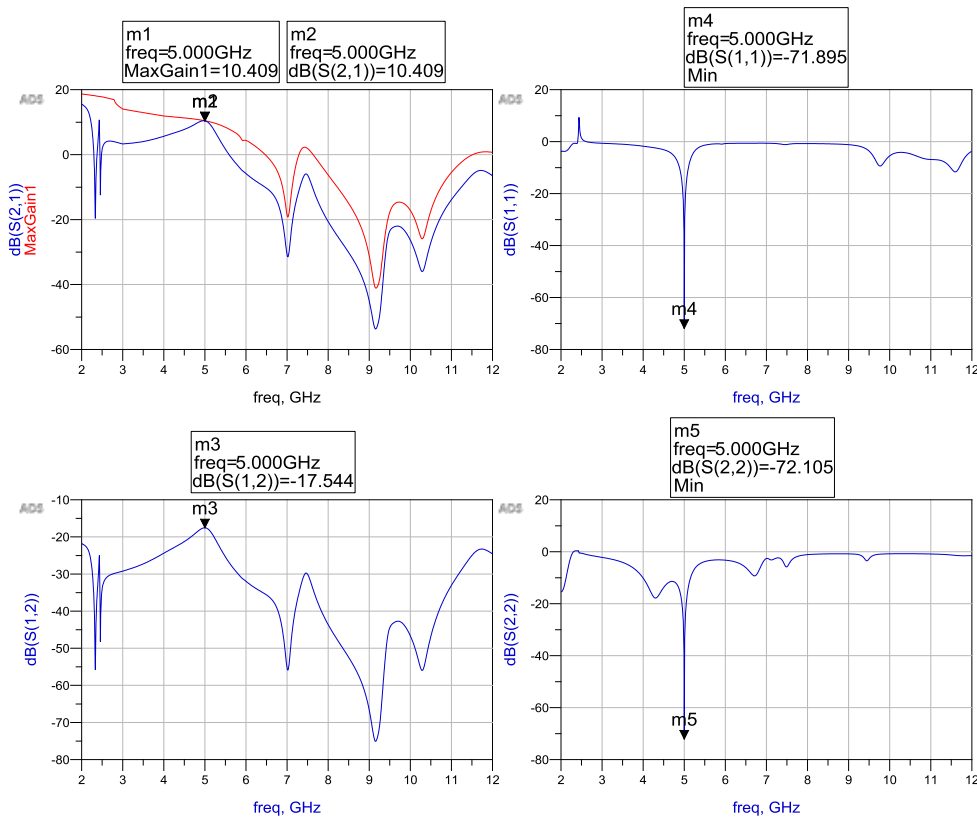


Fig. 26. S-Parameters from the maximum-gain amplifier.

3.5.2 EM-cosimulation design

Since we have completed with the schematic design and simulation of the maximum-gain amplifier, it was also suitable to do the EM-Cosimulation for the amplifier, in order to have more accurate results as compared to the schematic results. Since the amplifier is generated in a real layout to be able to simulate it. Thus, all components were placed again on this layout. As shown in Fig. 27.

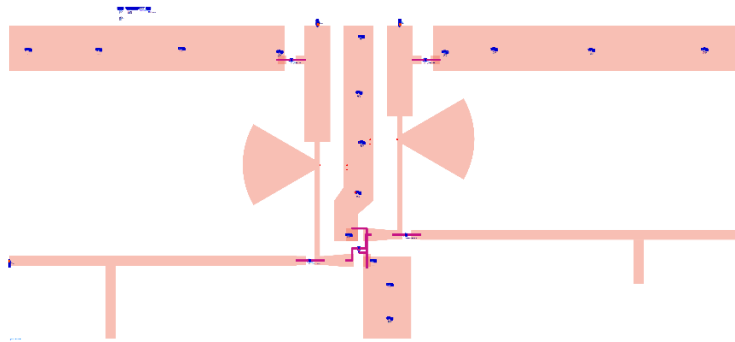


Fig. 27. Layout generated for the maximum-gain amplifier.

Fig. 28. shows the results obtained from EM-cosimulation of the layout generated for the maximum-gain amplifier, where the maximum gain achieved is 10 dB by the forward coefficient S_{21} , while S_{11} is -17.063 dB and S_{22} is -22.148 dB

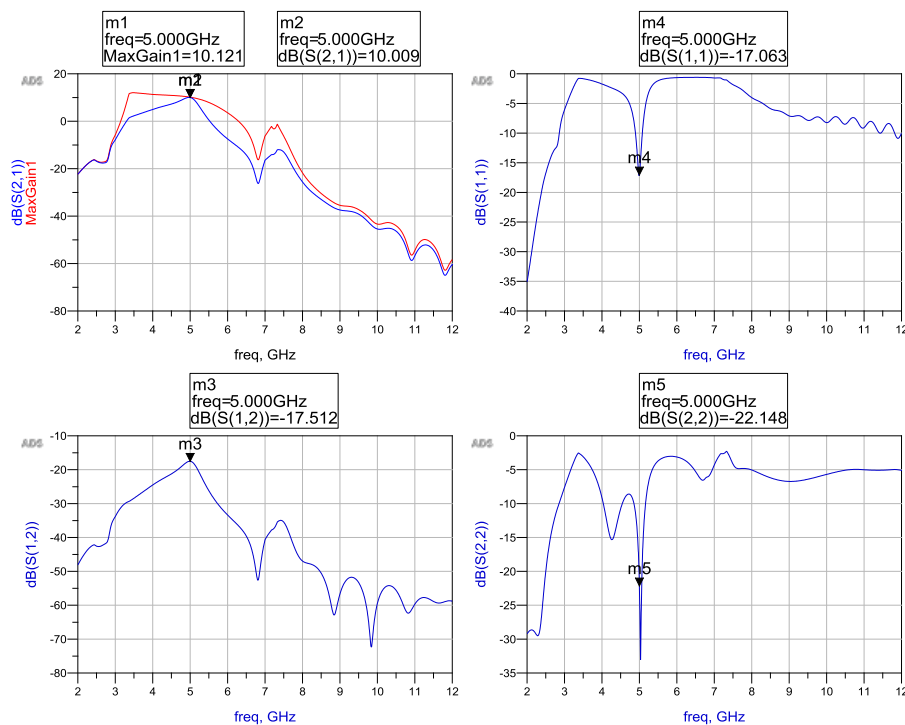


Fig. 28. EM-cosimulation results from the maximum-gain amplifier.

3.6 Minimum-noise amplifier

3.6.1 Schematic design

For this design, we will choose the same transistor due to it is ideal for minimum noise and high linearity behavior. Since we have changed the $\tan \delta$ parameter, the DC-bias network for the minimum-noise amplifier will be a little different from the DC-bias network for the maximum-gain amplifier, regarding the dimensions of the radial resonator and the quarter-wave transformer. Thus, in this design, we will consider the new $\tan \delta$ (0.042) parameter to design the whole minimum-noise amplifier. Therefore, the parameters characterized for the substrate will be as follow

$$\epsilon_r = 4.21 \quad ; \text{Dielectric constant}$$

$$\tan \delta = 0.042 \quad ; \text{Loss tangent}$$

As we can see in Fig. 29. the DC-bias network for the minimum-noise amplifier has been designed.

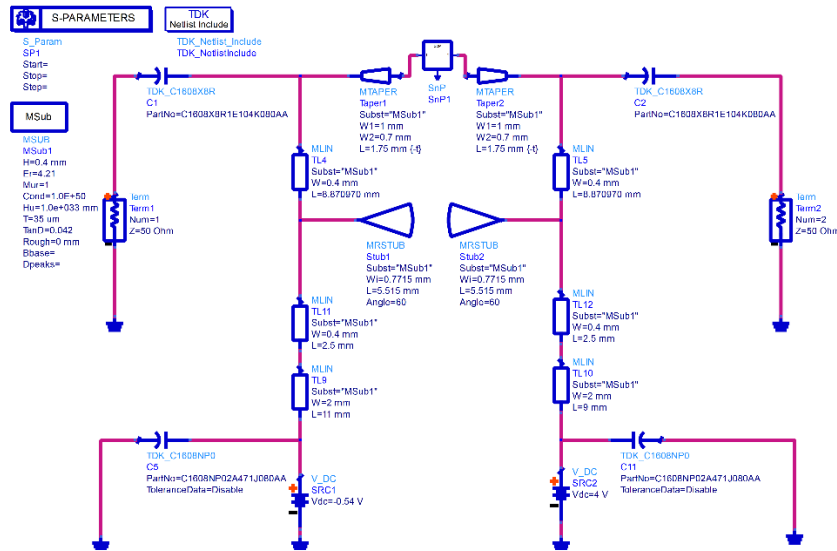


Fig. 29. DC bias network for the minimum-noise amplifier.

After doing the simulation of the DC-bias network for the minimum-noise amplifier, the stability factor given by *Rollet's condition* (k) is unconditionally stable due to $k = 1.051$. Then, we can do the matching networks for the transistor. Thus, in order to achieve the minimum

noise at the input of the transistor, we must set up $\Gamma_S = \Gamma_{opt}$, as we discussed in subsection 2.4.4, where ADS provide this optimum reflection coefficient as S_{opt}

And to be able to get the maximum gain achievable at the output of the transistor, it is necessary to satisfy $\Gamma_{out} = \Gamma_L^*$, which is given by

$$\Gamma_{out} = \left(S_{22} + \frac{S_{12}S_{21}S_{opt}}{1 - S_{11}S_{opt}} \right)^*$$

As we can see in Fig. 30. both reflection coefficients S_{opt} and Γ_L^* have been measured.

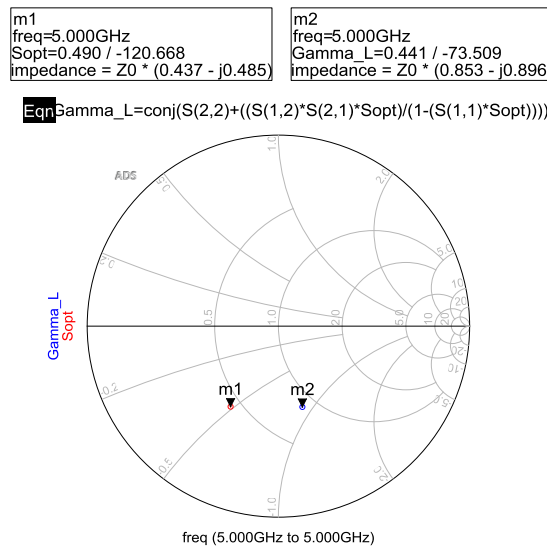


Fig. 30. Optimum and conjugate coefficients for the minimum-noise amplifier.

Since we have both reflection coefficient S_{opt} and Γ_L^* , we will match the amplifier by using the *Smith Chart* tool of ADS, since they will be in ideal transmission lines, we will convert them into microstrip lines by using *LineCal* tool.

where it will be also necessary to add two characteristic transmission lines (50Ω) at the input and output for the minimum-noise amplifier, in order to make the connection of SMA terminal. Then, an adjustment will be needed in the whole amplifier in order to avoid mismatch of the matching networks.

As we can see in Fig. 31. The matching networks for the minimum-noise amplifier have been designed.

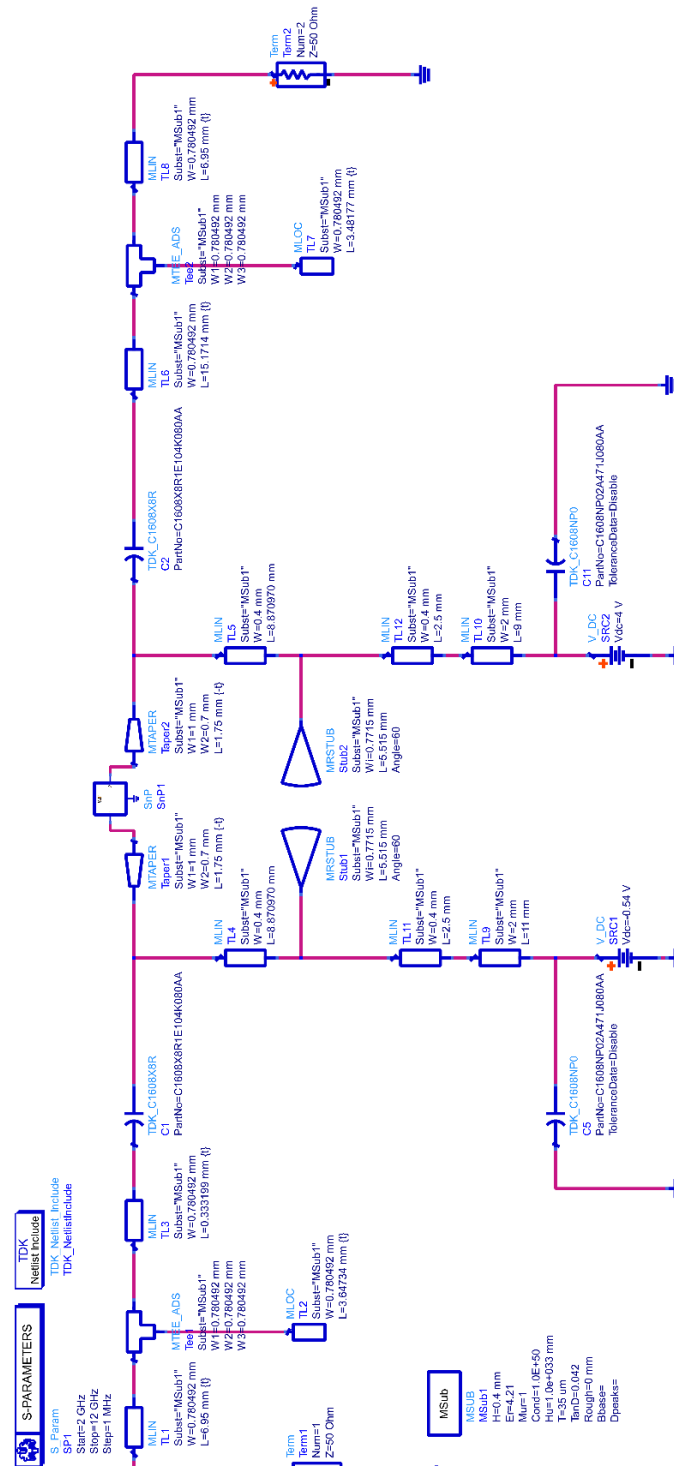


Fig. 31. Minimum-noise amplifier.

After the matching networks were fixed for the minimum-noise amplifier, we can notice that S_{opt} and Γ_L^* are placed in the center of the Smith chart, see Fig. 32.

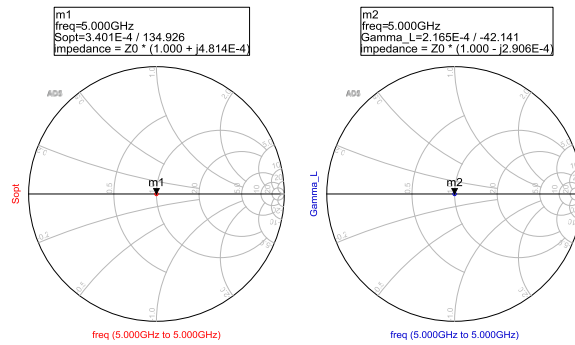


Fig. 32. Reflection coefficients matched for the minimum-noise amplifier.

Fig. 33. shows the results from the simulation of the minimum-noise amplifier, where the forward coefficient S_{21} is 7.769 dB, while, both reflection coefficients S_{opt} and Γ_L^* are well matched to get the minimum noise at the input and maximum gain at the output of the amplifier. Also, we can see that the input reflection coefficient S_{11} is not matched at all; this behavior of S_{11} is usual since we are matching the optimum coefficient S_{opt} at the input of the transistor instead of S_{11} .

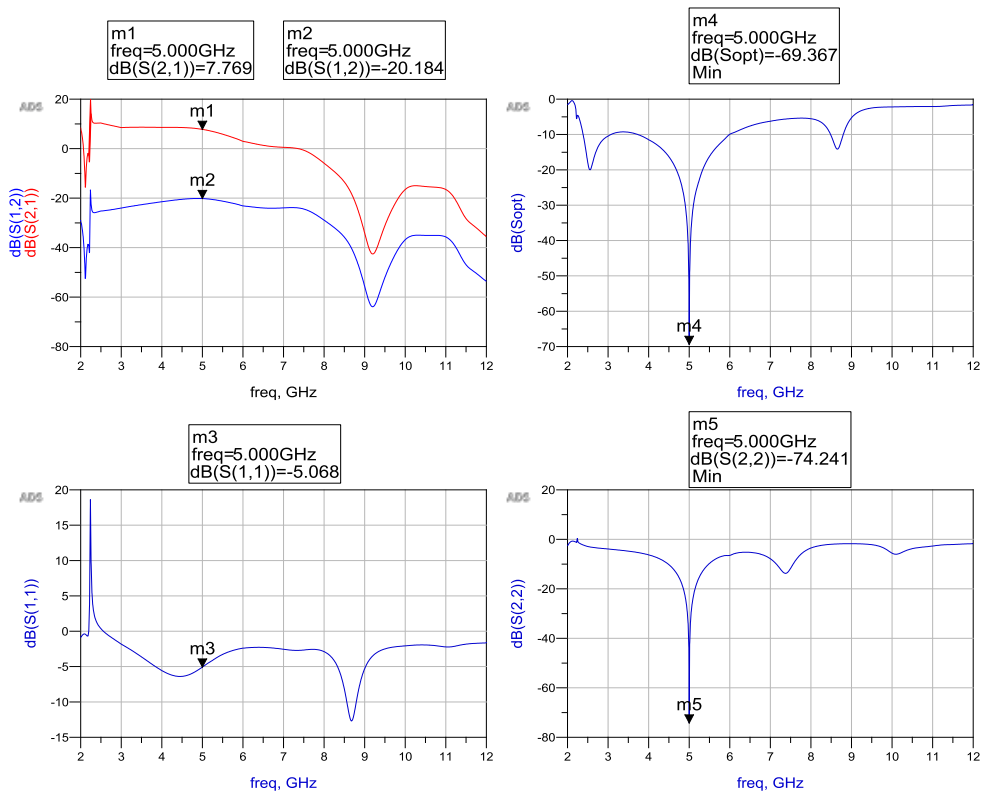


Fig. 33. S-parameters results from the minimum-noise amplifier.

Since this minimum-noise amplifier will be placed at the first stage of the cascaded amplifier, thus, the entire noise figure (NF) of the cascaded amplifier will be dominated by the first stage as we discussed in Subsection 2.4.5

As we can see in Fig. 34. The simulation of the minimum-noise amplifier is getting a noise figure of 1.217 dB since the matching network has been performed to get the minimum noise at the input of the amplifier, also the specific noise figure “nf(2)” provided by ADS is reaching this minimum noise.

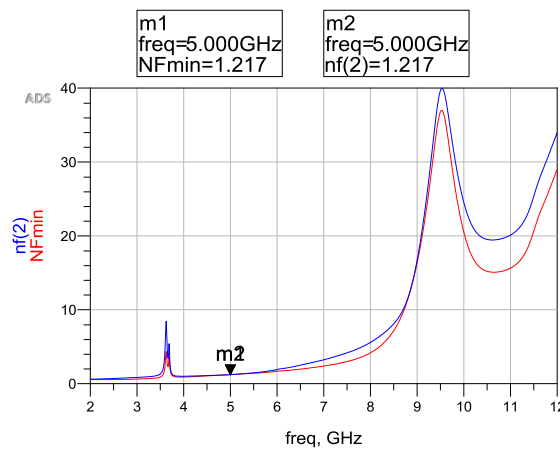


Fig. 34. Noise figure achieved from the amplifier.

3.6.2 EM-cosimulation design

To be able to have more accurate results from the minimum-noise amplifier, we performed the EM-cosimulation of it, in order to consider the schematic and electromagnetic simulations.

Fig. 35 shows the layout for the minimum-noise amplifier.

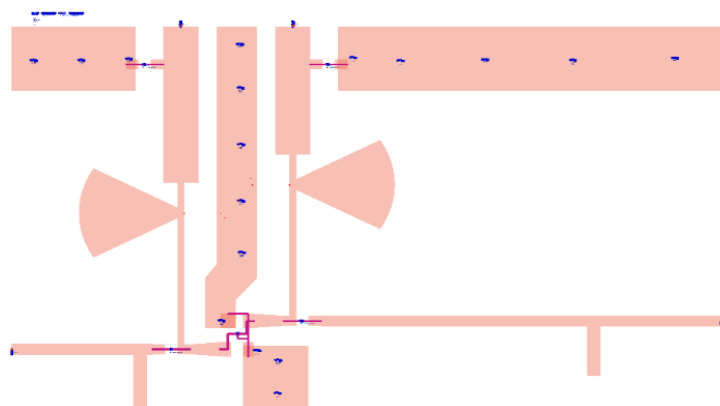


Fig. 35. Layout for the minimum-noise amplifier.

As we can see in Fig. 36. the EM-cosimulation results from the minimum-noise amplifier, where the optimum coefficient S_{opt} is -18.561 dB of attenuation, while S_{22} is -15.303 dB, thus, with these values, we are satisfying the necessary requirements to get the minimum noise from the amplifier.

Nevertheless, we got 7.942 dB gain, which is quite lower as compared to the maximum-gain amplifier.

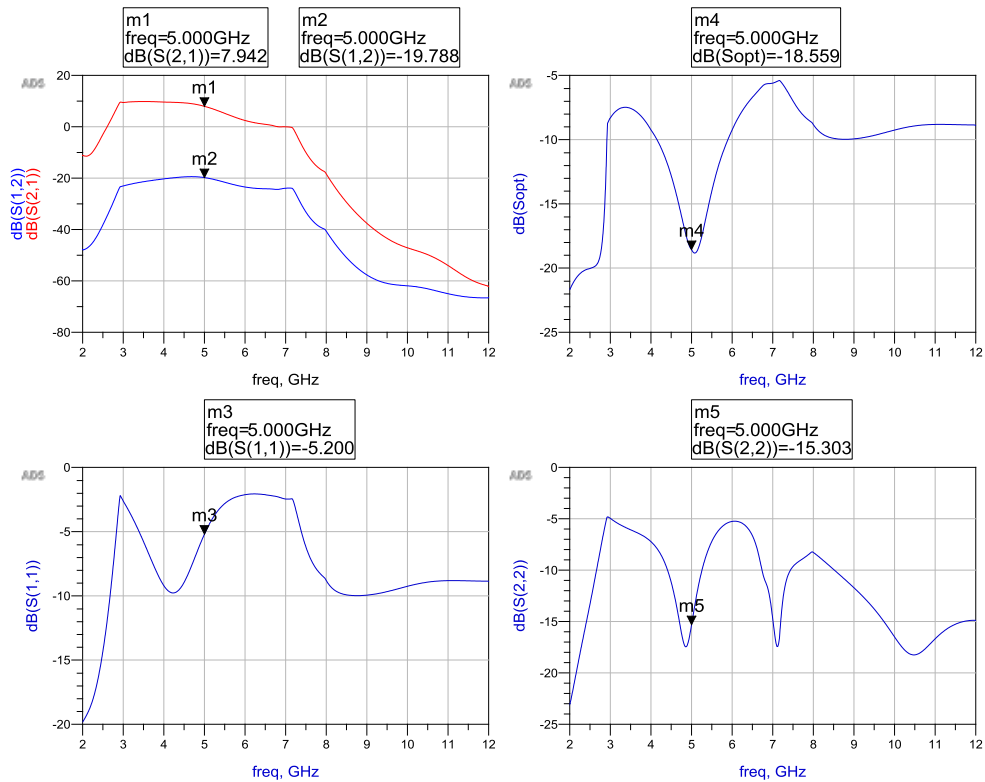


Fig. 36. EM-cosimulation results from the minimum-noise amplifier.

3.7 Design of two-stage LNA

To carry out this part of the project, it will be designed just as a software design, since the substrate used to make the manufacture of the amplifiers has a $\tan \delta$ more than a usual substrate.

3.7.1 First stage

Since we have designed each amplifier separately, in this step we will design a cascaded LNA in a single circuit. For this purpose, we will take the DC-bias networks from the previous design, in order to obtain the coefficients of S_{opt} and Γ_L^* for this first stage (minimum noise). As we have discussed before this configuration of the DC-bias is unconditionally stable.

Therefore, after doing the simulation of this DC-bias network, we can obtain the necessary coefficients to do the matching networks, which are given as follow

$$S_{opt} = 0.437 - j0.485$$

$$\Gamma_L^* = 0.853 - j0.896$$

3.7.2 Second stage

To be able to have the second stage of the cascaded amplifier working in maximum gain, it is necessary to apply the conjugate matching coefficients discussed in subsection 2.4.3, regarding having $\Gamma_{in} = \Gamma_s^*$ and $\Gamma_{out} = \Gamma_L^*$, since the DC-bias network is unconditionally stable as well, we can obtain these conjugate coefficients by fixing the conjugate equations in ADS, which are given as follow

$$\Gamma_s^* = 0.285 - j1.369$$

$$\Gamma_L^* = 0.331 - j0.557$$

3.7.3 Intermediate matching network

Since we have both DC-bias networks for the minimum noise and maximum-gain amplifier. In order to do the matching network between those amplifiers. We will take the output conjugate coefficient from the minimum-noise amplifier that is $0.853-j0.896$ and the input conjugate coefficient from the maximum-gain amplifier, which is $0.285-j1.369$, thus, we can do the matching network for those coefficients by using the Smith chart tools of ADS. And making

sure that one of those coefficients should be conjugated again in order to have the correct intermediate matching network. As shown in Fig. 37.

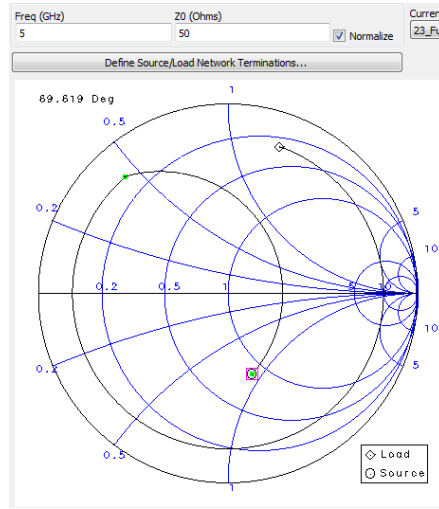


Fig. 37. Intermediate matching coefficients for the cascaded LNA.

Once we have completed with the intermediate matching coefficient, we must convert it into microstrip transmission lines.

As we can see in Fig. 38 the intermediate matching network has been converted into microstrip transmission lines.

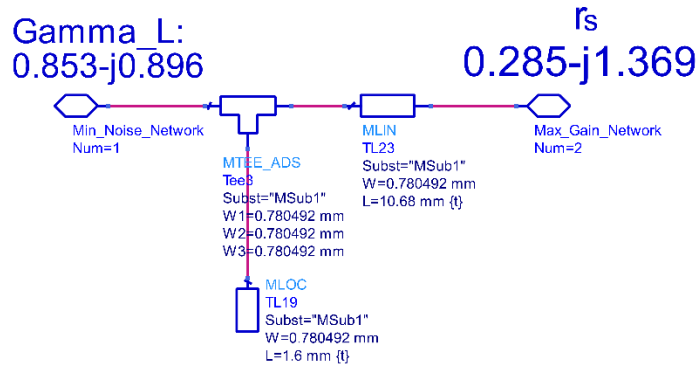


Fig. 38. Intermediate-matching network for the cascaded LNA.

3.7.4 Design of matching networks for the cascaded LNA

After fixing the intermediate matching network, we can match the input and output of the cascaded LNA, since we have the input coefficients, which is given by $S_{opt} = 0.437-j0.485$ (first stage) and $\Gamma_L^* = 0.331-j0.557$ (second stage). Thus, we placed both coefficients to the center of

the Smith chart. Where it was also necessary to do an adjustment in the whole amplifier since we added two characteristic transmission lines for the SMA terminals.

As we can see in Fig. 39 all matching networks have been designed.

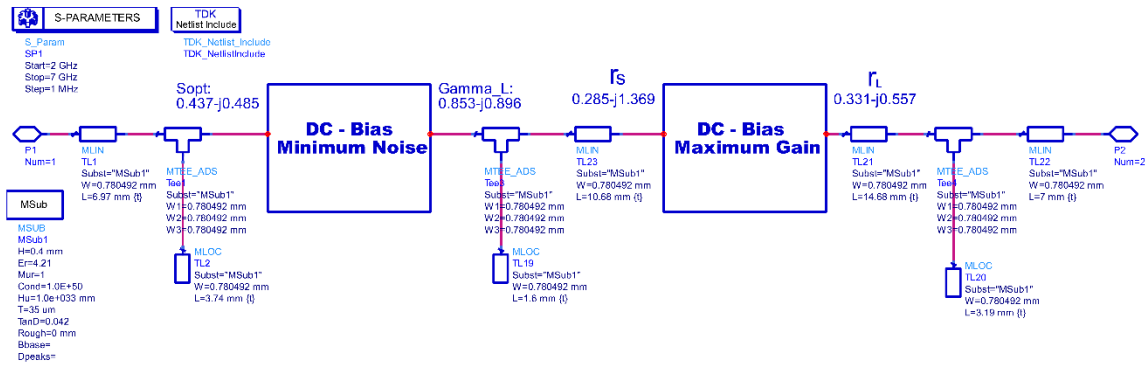


Fig. 39. Cascaded LNA.

Therefore, we can see in Fig. 40 that the matching networks are placing the coefficients S_{out} and Γ_L^* to the center of the Smith chart.

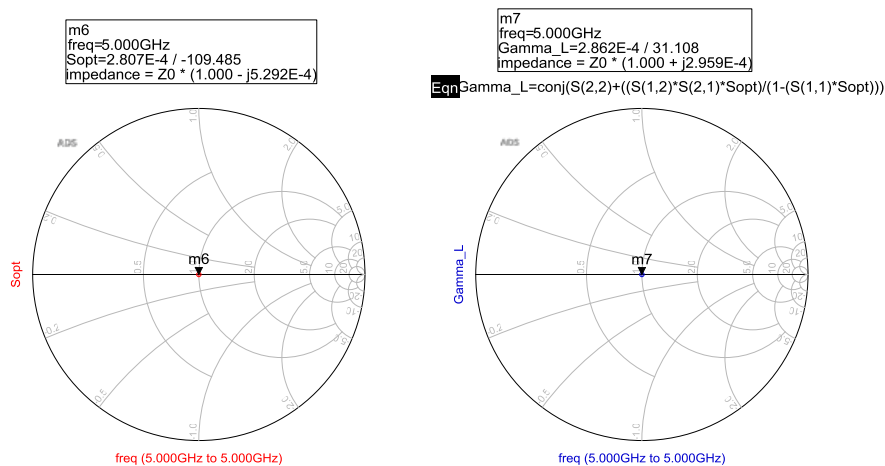


Fig. 40. Input and output coefficients matched.

Fig. 41 shows the results from the simulation of the cascaded LNA, where S_{21} is 14.961 dB of gain, also the optimum coefficient is -71 dB of attenuation and the output reflection coefficient S_{22} is -70 dB as well.

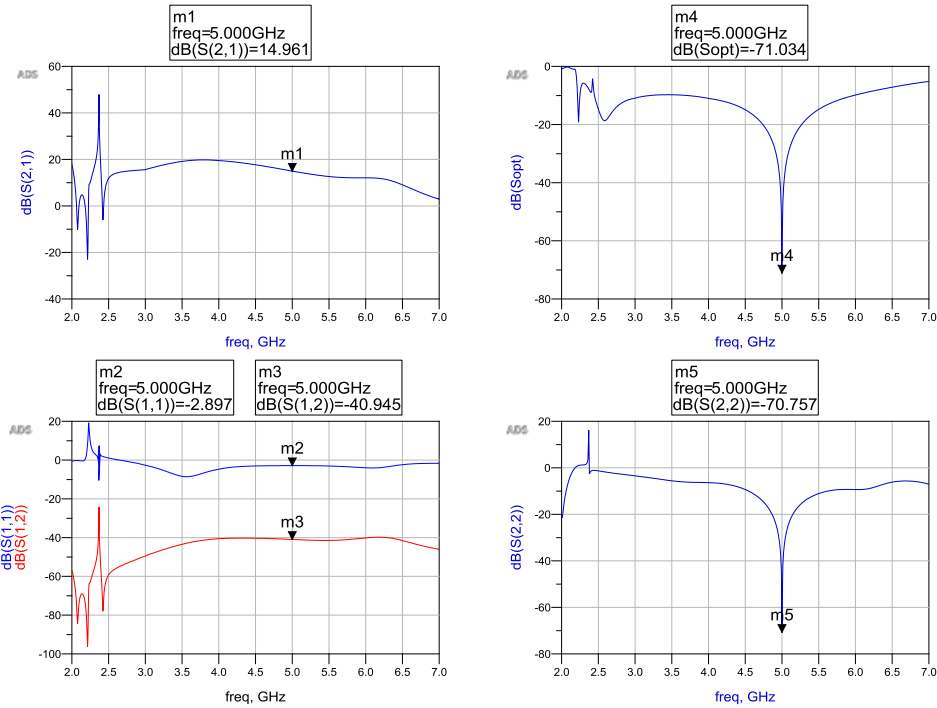


Fig. 41. Schematic results from the cascaded LNA.

Since the first stage from the cascaded LNA is designed to get the minimum noise, we can see that the overall noise figure is covered by the first stage, which is 1.293 dB of noise figure. As shown in Fig. 42.

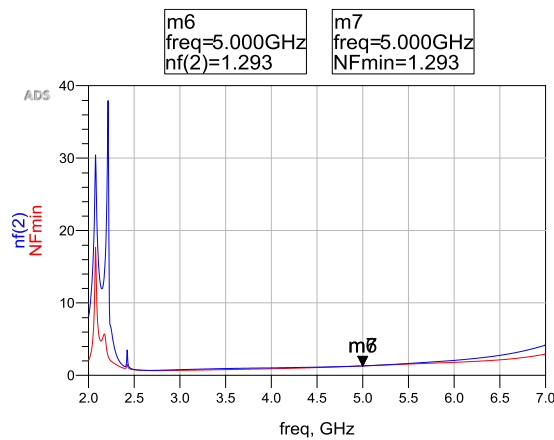


Fig. 42. Minimum-noise achieved from the cascaded LNA.

3.7.5 EM-cosimulation for the cascaded LNA.

In order to have more accurate results from the cascaded LNA, we performed the EM-cosimulation of it.

Fig. 43 shows the layout for the cascaded LNA.

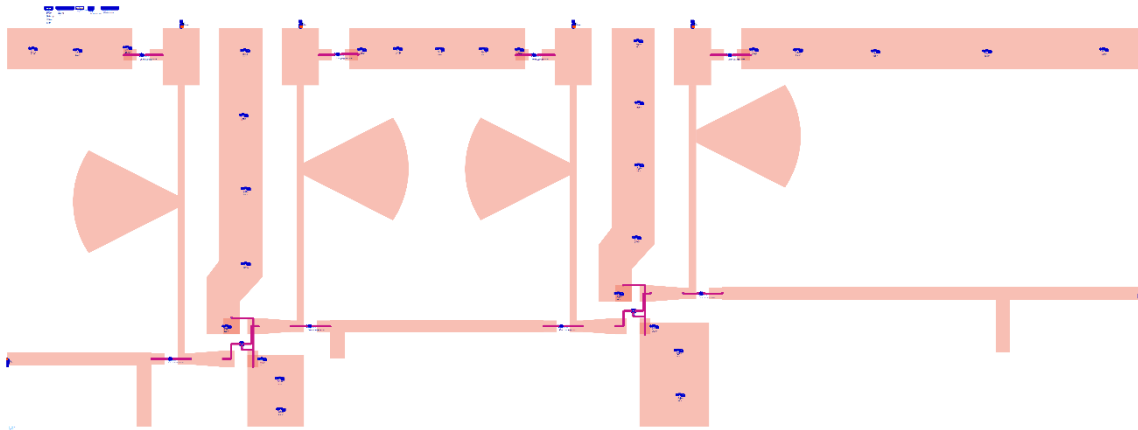


Fig. 43. Layout generated for the cascaded LNA.

Fig. 44 shows the results from the EM-cosimulation for the cascaded LNA.

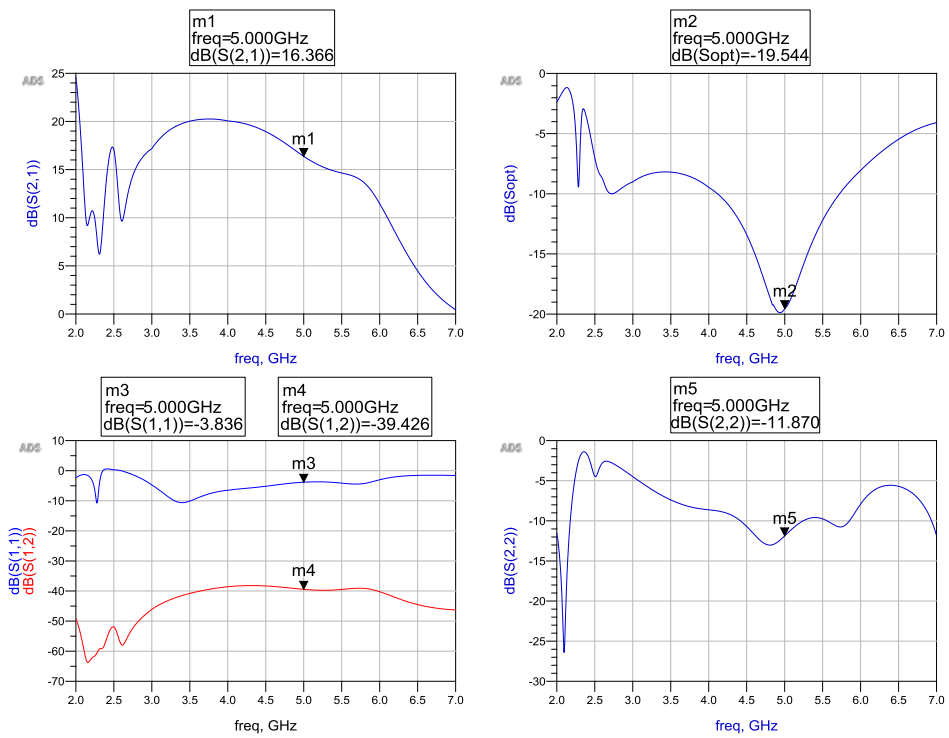


Fig. 44. EM-cosimulation results from the cascaded LNA.

4 Manufacturing

Since we have the layout of the amplifiers and the resonator design (characterization of the substrate), we performed the manufacture of them by using the insulator technique, following the below steps.

4.1 Insulator technique

- To be able to make the amplifiers, it was necessary to export them to the *Gerber* format in ADS. In order to print them on a transparency film for laser printers. As shown in Fig. 45.

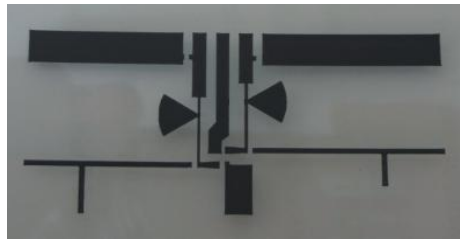


Fig. 45. Transparency film printed with the amplifier design.

- Since we have the transparency film of the amplifiers, they were exposed inside the insulator with the substrate for 160 seconds.
- Then a *Positive-Type Board Developer* concentration was used in order to check the design of the amplifier in the substrate.
- Finally, all components were placed on top of the substrate characterized with the soldering tin. Then the substrate was placed inside the programmable desktop reflow oven for 15 minutes to achieve 210 °C of temperature. As shown in Fig. 46.

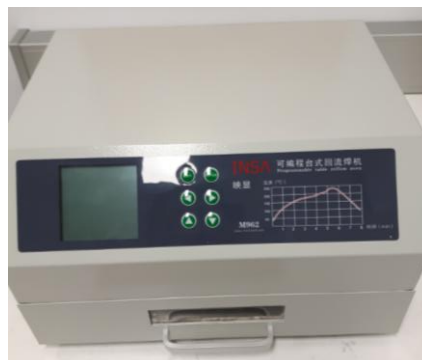


Fig. 46. Programmable desktop reflow oven.

5 Measurements

5.1 Measurements equipment

5.1.1 E8363B network analyzer

To perform the measurements of the circuits designed, we used the E8363B Vector Network Analyzer (VNA) in order to compare these results with the EM-cosimulation results. The measured results have saved as S2P file to be able to represent them in ADS.



Fig. 47. Vector Network Analyzer E8363B.

5.1.2 N4693A electronic calibration module

The calibration of the VNA was done by using the N4693A electronic calibration module (see Fig. 48), in order to measure the amplifiers over the desired range of frequency (2 GHz to 12 GHz). This operation was done with a simple one-connection operation to the module, which offers excellent accuracy without spending the time to calibrate the VNA.



Fig. 48. Electronic calibration module N4693A.

5.2 Maximum-gain amplifier

Fig. 49. shows the comparison between the EM-cosimulation results and VNA measurements, where the forward coefficient S_{21} measured is 7.629 dB. Nevertheless, the reflection coefficients S_{11} measured is -22.888 dB, which is even better than the EM-cosimulation result, also S_{22} measured is -17.021 dB. Thus, with these results obtained to get the maximum gain of the amplifier, we can see that doing the EM-cosimulation, we will get more accurate results that is going to look like VNA measurement.

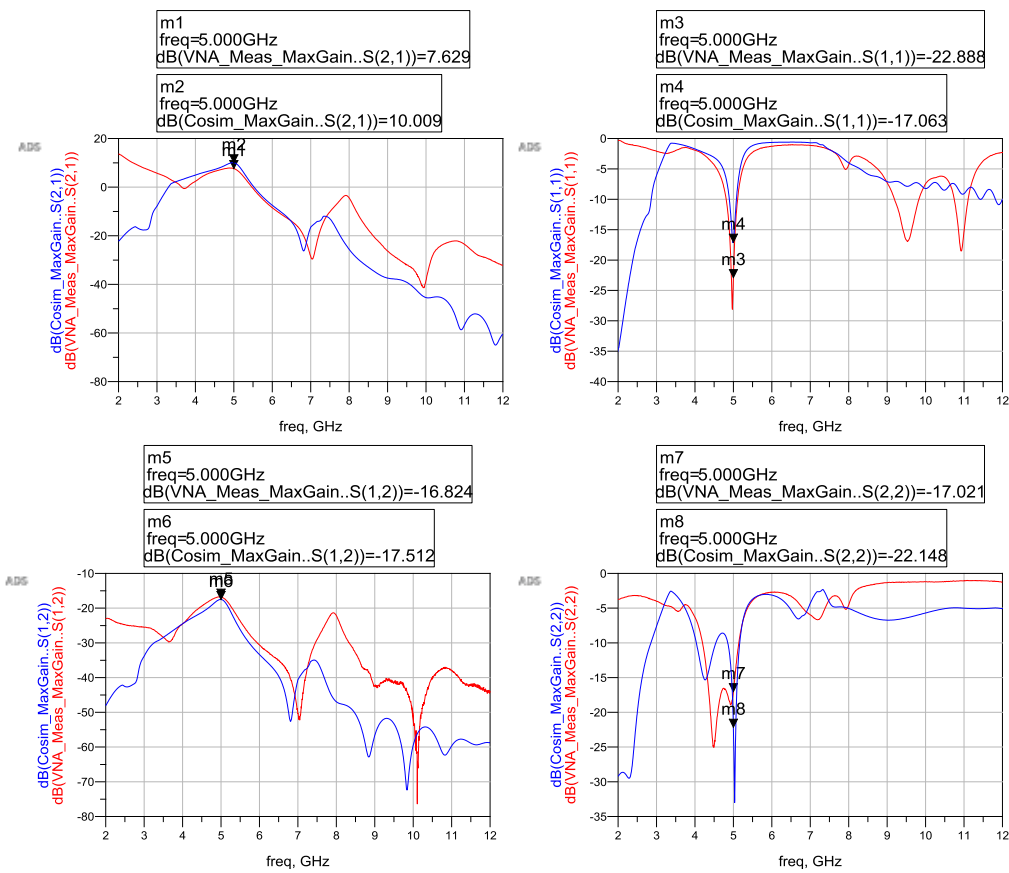


Fig. 49. Comparison between the EM-cosimulation results and VNA measurements.

5.3 Minimum-noise amplifier

Fig. 50. shows the comparison between the EM-cosimulation and VNA results, as we can see on it, the forward transmission coefficients S_{21} from the VNA measurement is 6.589 dB, which is lower than the EM-cosimulation result that was 7.942 dB, while the input reflection

coefficient (S_{11}) measured is -3.745 dB; since we designed this amplifier to get the minimum noise achievable by the amplifier, this input coefficient (S_{11}) will not be matched at all.

On the other side, the output reflection coefficient (S_{22}) measured is -13.163 dB that is matched well the amplifier, since we did the matching networks to get the maximum gain at the output of the amplifier.

Therefore, the comparison between the EM-cosimulation and VNA measurement have been done.

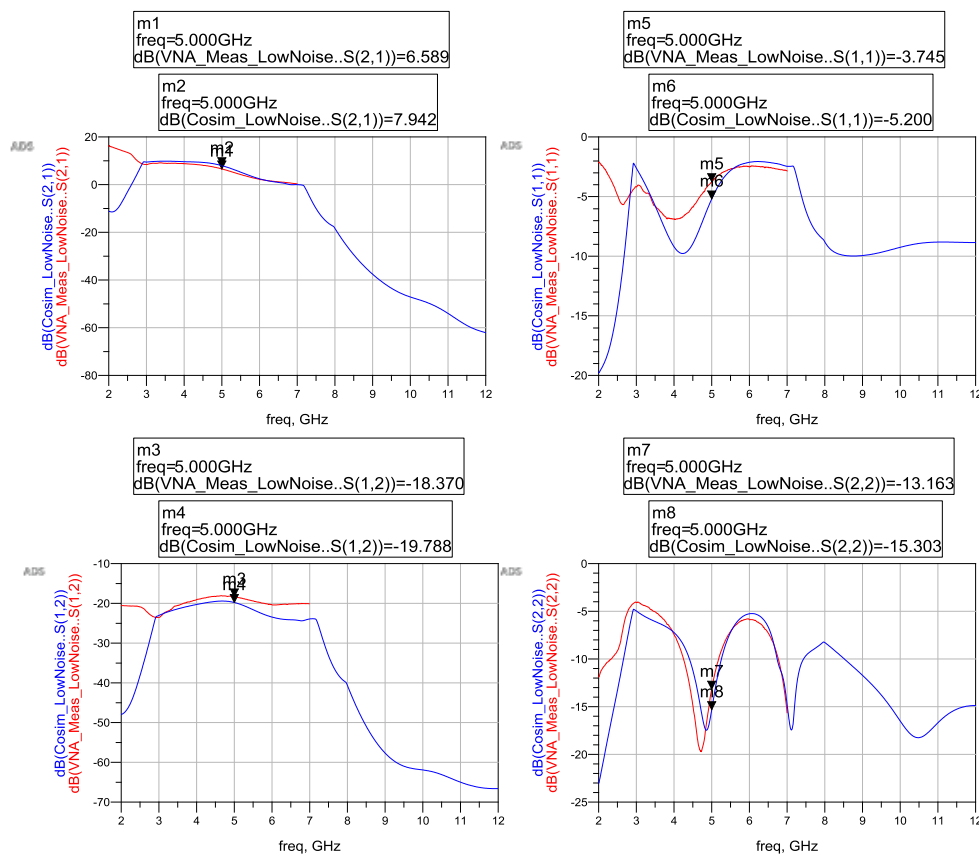


Fig. 50. Comparison between the EM-cosimulation results and VNA measurements.

5.4 Minimum noise and maximum-gain amplifier

To be able to do the measurement of the two amplifiers designed, it was necessary to use an attenuator of 3 dB, since we have noticed from the schematic simulation results that at lower frequencies from the fundamental frequency (5 GHz), the input reflection coefficient (S_{11}) was reflecting the RF-signal, this phenomenon is given by the transistor; since the stability condition

is frequency dependent, thus, at lower frequencies our DC-bias networks are not unconditionally stable.

Fig. 51. shows the measurements from the minimum noise and maximum-gain amplifiers, setting up in cascaded, where the forward transmission coefficient (S_{21}) measured is 9.425 dB, but taken into consideration the attenuator value of 3 dB, thus, we are getting 12.425 dB of gain.

Since the first amplifier was designed to get the minimum noise, the input reflection coefficient (S_{11}) of the cascaded amplifier is -3.581 dB, also, as we discussed in subsection 2.4.4 the first stage amplifier will dominate the noise figure for the two amplifiers, regarding *Friis's equation*. And, the output reflection coefficient (S_{22}) from the cascaded amplifier is -17.247 dB which is matching well the amplifier, since we did the conjugate matching at the output for the maximum-gain amplifier.

Then, in order to get the minimum noise figure achieved from the cascaded amplifiers, we did the EM-cosimulation, where it was 1.35 dB of noise figure.

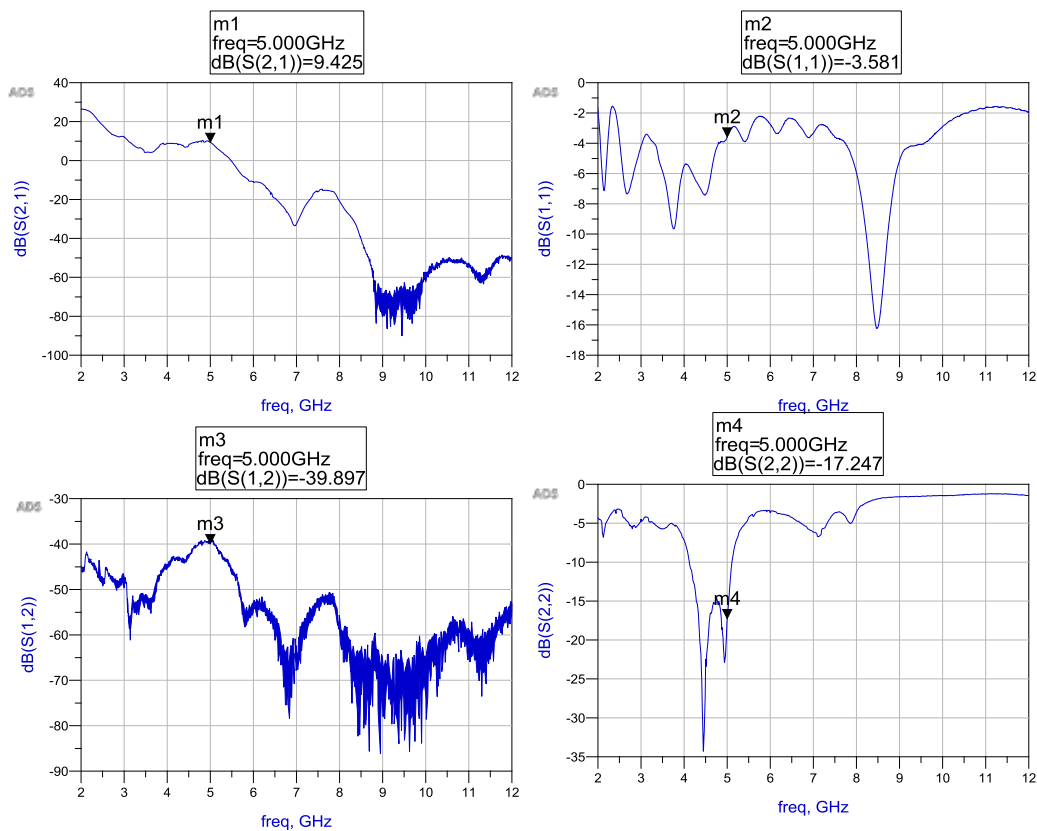


Fig. 51. VNA measurement of the two-stage amplifier.

6 Discussion

Characterization of the substrate

We performed the characterization to have accurate values of *the relative dielectric constant* (ϵ_r) and $\tan \delta$ of the substrate. We noticed that there are differences between parameters provided by the manufacturer and the real parameters. Where these parameters are really important is at the time when we are designing an application with active components because the dielectric constant has a relationship with the design frequency, thus, if we wrongly take this parameter, our expected result will be shifted in frequency, meaning also bad attenuation of the reflection coefficients. And on the other hand, the $\tan \delta$ is more related to the gain. Since the thickness (H) of the substrate used in this project was really thin, it does not mean that it is better than the usual substrate, as we have seen in our amplifier design.

Table 1. Parameters characterized for the substrate.

Parameter	Manufacturer	Characterization
ϵ_r	4.4	4.21
H	0.4 mm	0.4 mm
$\tan \delta$	0.02	0.042
T	35 μm	35 μm

Maximum-gain amplifier

At the beginning of this amplifier design, we considered the new *relative dielectric constant* (ϵ_r) for the substrate, since our results were not shifted to the design frequency, but the $\tan \delta$ (0.02) used to design it was wrong, which affected the gain of the amplifier, since, in the schematic and EM-cosimulation results, we obtained 10 dB gain, while from the VNA measurements was 7.629 dB. And for the input and output reflection measured, we obtained more than 15 dB of attenuation, which implies that the matching networks were well designed. Also, the bandwidth achieved for this amplifier was around 295 MHz, which was taken from the S_{11} reflection coefficient at 10 dB of attenuation.

Table 2. S-parameters obtained from the maximum-gain amplifier.

S-parameters	Schematic (dB)	Cosimulation (dB)	VNA (dB)
S21	10.409	10.009	7.629
S12	-17.544	-17.512	-16.824
S11	-71.895	-17.063	-22.888
S22	-72.105	-22.148	-17.021

Minimum-noise amplifier

To design this minimum-noise amplifier, we used the $\tan \delta$ (0.042) characterized, where the gain measured was 6.589 dB also the coefficient S_{11} measured was -3.745 dB, which seems like is not matching well the amplifier, because instead to use this coefficient S_{11} , the optimum coefficient S_{opt} was taken into account in order to have the minimum noise figure at the input of this amplifier.

Thus, the minimum noise figure achieved from the simulation of this amplifier was 1.217 dB, which is a little bit more than the expected results, which was less than 1 dB, it is clear the substrate used to make the amplifier is affecting the expected results, nevertheless we will measure both amplifiers characterized in order to get the gain and noise figure of the cascaded LNA.

Table 3. S-parameters obtained from the minimum-noise amplifier.

S-parameters	Schematic (dB)	Cosimulation (dB)	VNA (dB)
S21	7.769	7.942	6.589
S12	-20.184	-19.788	-18.370
Sopt	-69.367	-18.559	
S22	-74.241	-15.303	-13.163
S11	-5.068	-5.200	-3.745

Measurement of both amplifiers designed

Before to do the measurements of the amplifiers, it must be stated that at lower frequencies both amplifier have unwanted signals (reflections) on input reflection coefficient S_{11} , which is clearly seen in Fig. 26 and Fig. 33, this behavior was due to the stability condition which is

frequency dependent, thus, the testing for unconditional stability given by Rollet’s condition (K) at those frequencies are less than one, therefore, the amplifiers are unstable at those lower frequencies.

Since we got unwanted signals at frequencies lower than the fundamental frequency (simulation results), we used an attenuator of 3 dB, to be able to measure both amplifiers, where the gain obtained considering also the attenuator value was 12.425 dB, also it is clear that the first stage is dominating the whole system, because S_{11} remains as the previous measurement of the single minimum-noise amplifier, where the minimum noise figure achieved was 1.35 dB, which was getting from the EM-cosimulation of the two-stage amplifier designed.

Table 4. S-parameters obtained from the two stage amplifiers.

S-parameters	VNA (dB)
S21	9.425
S12	-39.897
S11	-3.581
S22	-17.247

Design of a Cascaded LNA

Cascaded LNA was performed in order to compare with the amplifiers manufactured (minimum noise and maximum gain), but this cascaded LNA was done just as in the software design and as a single design. As we notice in Table 5. The gain obtained for this cascaded LNA is reaching 16.366 dB, while S_{11} remains at -3.836 dB, where S_{opt} is well matched to get the minimum noise at the input of the amplifier, also the output coefficient S_{22} is well matched.

Table 5. EM-cosimulation results from the cascaded amplifier

S-parameters	Schematic (dB)	EM-Cosimulation (dB)
S21	14.961	16.366
S12	-40.945	-39.426
Sopt	-71.034	-19.544
S22	-70.757	-11.870
S11	-2.897	-3.836

Gain compression.

To carry out this measurement to find the 1 dB gain compression from the amplifier manufactured (maximum gain). We used the VNA to generate a sweep of power in it, thus, this power was introduced to the input of the amplifier. Where we got for input power at 8.5 dBm the gain of the amplifier, which was 7.629 dB gain, it reduced in 1 dB gain, therefore the gain compression occurred at 8.5 dBm of input power, thus, the output power from the amplifier will be at 16.229 dBm.

7 Conclusions

Minimum noise and maximum gain amplifiers have been designed and manufactured by using the ATF-34143 transistor in an unconditionally stable region at 5 GHz. Setting up in a cascaded the minimum noise and maximum-gain amplifier provided a noise figure of 1.35 dB and 12.425 dB gain at the fundamental frequency.

With these results, we could not cover the goal fixed at the beginning of this project due to the gain is less than the expected result (more than 20 dB) and the minimum noise figure achieved was 1.35 dB, which is more than the expected result (less than 1dB). Nevertheless, the gain and noise figure characterized are acceptable, since more commercial LNA for radar applications have more than 20 dB gain with a noise figure around 1.3 dB to 1.7 dB. Also, we have to consider that to develop this project, we used cheaper components like the transistor and the substrate, which also influenced with the results obtained.

In a future work, in these kinds of applications could be done better by using suitable components, of which one of them should be the substrate, nowadays, there is available the Rogers substrate (RO4003) with a $\tan \delta$ parameter of 0.001 given by the manufacturer. Also, to avoid unwanted signals close to the fundamental design frequency, it is convenient to place a band pass filter in order to have just the desired range of frequency.

References

- [1] D. M. Pozar, "Microwave Engineering", 4th ed., John Willey & Sons, Inc., 2012, p. 1.
- [2] R. E. Collin, "Foundations for Microwave Engineering", 2nd ed., John Willey & Sons, Inc., 2001, p. 3.
- [3] P. Tait, "Introduction to Radar Target Recognition", the Institution of Engineering and Technology, IET Radar Series n° 18, 2005, p. 55.
- [4] M. Golio, J. Golio, "RF and Microwave Applications and Systems", 2nd ed., Taylor & Francis Group, LLC, 2008, p. 17.
- [5] D. Fisher, I. J. Bahl, "Gallium Arsenide IC Applications Handbook", vol. 1, Academic Press, Inc., 1995, pp. 80-83.
- [6] A. F. Peterson, G. D. Durgin, "Transient Signals on Transmission Lines: An Introduction to Non-Ideal Effects and Signal Integrity Issues in Electrical Systems", Morgan & Claypool, 2009, pp. 3-7.
- [7] M. Steer, "Microwave and RF Design a Systems Approach", SciTech Publishing, Raleigh, NC., 2010, pp. 299-300.
- [8] I. J. Bahl, "Fundamentals of RF and Microwave Transistor Amplifiers", John Wiley & Sons, Inc., 2009, pp. 23-24.
- [9] B. Henderson, E. Camargo, "Microwave Mixer Technology and Applications", Artech House, 2013, pp. 81-82.
- [10] V. J. Kuhn, AlGaIn/GaN-HEMT Power Amplifier with Optimized Power-Added Efficiency for X-Band Applications, KIT Scientific Publishing, 2010, pp. 9-10
- [11] S. C. Cripps, "RF Power Amplifiers for Wireless Communications", 2nd ed., Artech House, 2006, p. 104.
- [12] M. Božanić, S. Sinha, "Power Amplifiers for S-, C-, X- and Ku-Bands: an EDA Perspective", Springer International Publishing Switzerland, 2016, p. 162.

Appendix A

Measurement of S-parameters for the maximum-gain amplifier.

As we can see in Fig. A1. The maximum-gain amplifier was measured by using the VNA with a suitable DC supply for the transistor (ATF-34143). And to carried out this process, it was necessary to calibrate the VNA in order to have the desired range of frequency. The power DC supply (3631A) was used to bias the transistor with an accurate DC supply.

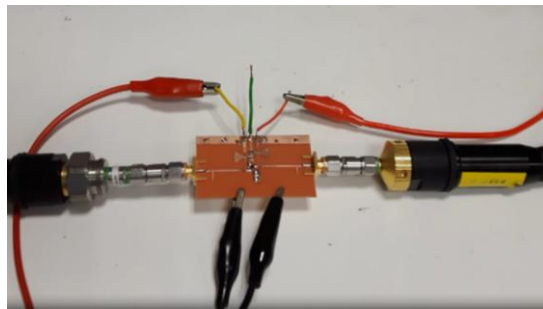


Fig. A1. Measurements of the maximum-gain amplifier.

Fig. A2. Shows the S-parameters obtained from the maximum-gain amplifier.

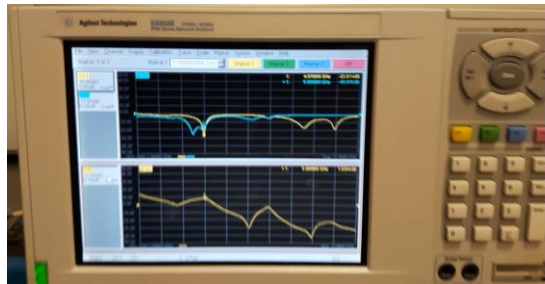


Fig. A2. S-parameters from the maximum-gain amplifier.

Fig. A3 shows the amplifiers manufactured and the resonator circuit to characterize the substrate.

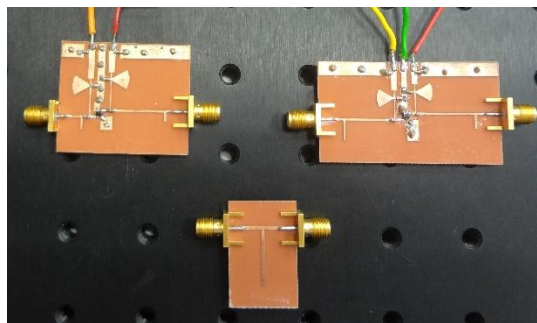


Fig. A3. Circuits characterized.